Solitons in Cellular Neural Networks

Makoto Itoh [1]
1-19-20-203, Arae, Jonan-ku,
Fukuoka, 814-0101 JAPAN
Email: itoh-makoto@jcom.home.ne.jp

Abstract
The two-dimensional autonomous cellular neural networks (CNNs) having one layer or two layers of memristor coupling can exhibit many interesting nonlinear waves and bifurcation phenomena. In this paper, we study the nonlinear waves (solitons) in the one-dimensional CNN *difference equations*. From our computer simulations, we found that the CNN difference equations can exhibit many interesting behaviors. The most remarkable thing is that the first-order *linear* CNN difference equation can exhibit a train of *solitary* waves, if the initial condition is given by the *unit step function*. Furthermore, the second-order *linear* CNN difference equation can exhibit *soliton-like* behavior, if the initial condition is given by a *pulse wave*. That is, the solitary waves pass through one another and emerge from the collision. Furthermore, the solution exhibits the *area-preserving behavior*, and it returns exactly to its initial state (the *recurrence of the initial state*). In the case of the *nonlinear* CNN difference equation, we observed the following interesting behaviors. In the Korteweg-de Vries CNN difference equation, the three-dimensional plot of the interaction of the solitary waves looks like a *chicken cockscomb*. In the Toda lattice CNN difference equation, a *train* of solitary waves with a *negative* amplitude interact with a *train* of solitary waves with a *positive* amplitude, and they emerge from the collisions. Furthermore, after a certain period of time, the solution breaks down. In the Sine-Gordon CNN difference equation, the solution moves at constant speed, and it emerges from the collision. Furthermore, the solution returns the state which is roughly similar to the initial state. In the *memristor* CNN difference equations, the three-dimensional plots of solitary waves exhibit more complicated (chaotic or distorted) behavior.

Keywords
soliton; nonlinear wave; CNN difference equation; memristor; first order wave equation; second order wave equation; Korteweg-de Vries (KdV) equation; Sine-Gordon equation; Toda lattice equation.; central difference scheme.

1 Introduction

A soliton is a solitary wave (a wave packet or pulse) that behaves like a particle, and its amplitude, shape, and velocity are conserved after a collision with another soliton. In most cases, a soliton satisfies the following conditions [1]:

1. It must maintain its shape when it moves at constant speed.
2. When a soliton interacts with another soliton, it emerges from the collision unchanged except possibly for a phase shift.

[1] After retirement from Fukuoka Institute of Technology, he has continued to study the nonlinear dynamics on memristors.

In this paper, we study the *solitons* of the CNN *difference equations*, which can satisfy the above conditions. We first consider several one-dimensional CNN circuit equations, and we obtain the difference equations from these equations by using the *central difference scheme*. The above CNN difference equations are equivalent to the discretized equations of well-known soliton equations. We next derive the *meristor* CNN circuit models by replacing a basic circuit element of the CNN circuit models by a *memristor*. Similarly, we can obtain the memristor CNN difference equations by using the central difference scheme.

In this paper, we give a unit step function or a pulse wave as the initial condition, besides the sine and cosine functions. From our computer simulations, we found that the CNN difference equations (CNN Diff. Eqs.) exhibit the following interesting behaviors:

(1) First-order *linear* wave CNN Diff. Eq.
A train of *solitary* waves are generated, if the initial condition is given by the *unit step function*. However, the initial wave moves at a constant speed *without distortion*, if the initial condition is given by the *sine function*

(2) First-order *nolinear* wave CNN Diff. Eq.
The shape of the initial curve is distorted continuously with increasing time, if the initial condition is given by the *sine wave*. The wave gets progressively steeper until the wave overtops, and ultimately the waveform breaks down.

(3) Second-order *linear* wave CNN Diff. Eq.
A solution can exhibit *soliton-like* behavior, that is, it moves at constant speed, and it emerges from the collision, if the initial condition is given by a *pulse wave*. Furthermore, the solution exhibits the *area-preserving* behavior, and returns exactly to its initial state, that is, the *recurrence of the initial state* is observed.

(4) Korteweg-de Vries (KdV) CNN Diff. Eq.
A solution evolves into a train of soliton waves, if the initial condition is given by the function of tangent hyperbolic. Furthermore, the three-dimensional plot of the interaction of the soliton waves looks like a *chicken cockscomb*, if the initial condition is given by the *cosine wave*.

(5) Sine-Gordon CNN Diff. Eq.
The behavior of the solution is quite similar to that of the second-order linear wave CNN difference equation, but its shape is distorted, if the initial condition is given by a *pulse wave*. The solution moves at constant speed, and it emerges from the collision. Furthermore, the solution returns the state which is roughly similar to the initial pulse.

(6) Toda lattice CNN Diff. Eq.
A train of solitary waves with *negative* (res. positive) amplitude interact with a train of solitary waves with a *positive* (res. negative) amplitude, and they emerge from the collisions, if the initial condition is given by a *sine wave*. Furthermore, after a certain period of time, the solution breaks down.

Furthermore, in the case of the *memristor* CNN difference equations, the three-dimensional plots of soliton waves exhibit more complicated (chaotic or distorted) behavior.

2 Wave Equations

2.1 Second-order wave equation

The wave equation for a plane wave traveling in the x direction on an interval $[0, L]$ is

Second-order wave equation

$$\frac{\partial^2 u(x,t)}{\partial t^2} = a^2 \frac{\partial^2 u(x,t)}{\partial x^2}, \tag{1}$$

where $u(x,t)$ is the amplitude of the wave at position x and time t, and a is the velocity of the wave. The general solution of Eq. (1) is given by

$$u(x,t) = \varphi(x+at) + \psi(x-at), \tag{2}$$

where $\varphi(x)$ and $\psi(x)$ are arbitrary functions that are continuously differentiable at least twice for all x.

2.1.1 Initial conditions

In this paper, we consider the following initial conditions:

$$\left.\begin{aligned} u(x,t)\Big|_{t=t_0} &= f(x), \\ \frac{\partial u(x,t)}{\partial t}\Big|_{t=t_0} &= 0, \end{aligned}\right\} \tag{3}$$

which specify the initial position and velocity for Eq. (1). Let $\phi(x,t)$ be a solution of Eq. (1). Then it has to satisfy

$$\phi(x,t_0) = f(x). \tag{4}$$

Thus, the function $f(x)$ should be continuously differentiable at least twice for all x on L, since Eq. (1) is the second-order partial differential equation.

2.1.2 Boundary conditions

We consider the two typical boundary conditions for Eq. (1):

- Dirichlet (fixed) boundary condition: $u(0,t) = d$ and $u(L,t) = e$ (d and e are constants).
- Periodic boundary condition: $u(0,t) = u(L,t)$.

2.1.3 Approximating the wave equation

We approximate Eq. (1) by using the central difference scheme. Let us define u_j^n by

$$u_j^n \stackrel{\text{def}}{=} u(x_j, t_n), \tag{5}$$

where $x_j = x_0 + j\Delta x$ and $t_n = t_0 + n\Delta t$ (x_0, t_0, Δx, and Δt are some constants, and j and n are integers). Using a *second-order central difference* for the space and time derivatives, we obtain:

$$\begin{aligned} \frac{\partial^2 u(x,t)}{\partial x^2}\Big|_{t=t_n,\, x=x_j} &\approx \frac{u(x_{j+1},t_n) - 2u(x_j,t_n) + u(x_{j-1},t_n)}{(\Delta x)^2} = \frac{u_{j+1}^n - 2u_j^n + u_{j-1}^n}{(\Delta x)^2}, \\ \frac{\partial^2 u(x,t)}{\partial t^2}\Big|_{t=t_n,\, x=x_j} &\approx \frac{u(x_j,t_{n+1}) - 2u(x_j,t_n) + u(x_j,t_{n-1})}{(\Delta x)^2} = \frac{u_j^{n+1} - 2u_j^n + u_j^{n-1}}{(\Delta t)^2}, \end{aligned} \tag{6}$$

where $|\Delta x|$ and $|\Delta t|$ are sufficiently small. Then, we can approximate Eq. (1) by the following difference equation:

Difference equation for Eq. (1)

$$u_j^{n+1} - 2u_j^n + u_j^{n-1} = \frac{(\Delta t)^2}{(\Delta x)^2}\, a^2 \left(u_{j+1}^n - 2u_j^n + u_{j-1}^n\right), \tag{7}$$

or equivalently

$$u_j^{n+1} = 2u_j^n - u_j^{n-1} + \frac{(\Delta t)^2}{(\Delta x)^2}\, a^2 \left(u_{j+1}^n - 2u_j^n + u_{j-1}^n\right). \tag{8}$$

2.1.4 Calculation of initial states

The equation (8) for $n = 2$ can be written as

$$u_j^2 = 2u_j^1 - u_j^0 + \frac{(\Delta t)^2}{(\Delta x)^2}\, a^2 \left(u_{j+1}^1 - 2u_j^1 + u_{j-1}^1\right). \tag{9}$$

In oder to obtain u_j^2 ($n = 1$) from Eq. (9), we need to know the value of u_j^1, u_j^0, u_{j+1}^1, and u_{j-1}^1.

Let us first obtain the value of u_j^1. Consider the first equation of Eq. (3) for $x = x_j$. It can be described as follow:

$$u(x_j, t)\Big|_{t=t_0} = u(x_j, t_n)\Big|_{n=0} = u_j^n\Big|_{n=0} = u_j^0 = f(x_j), \tag{10}$$

where $u_j^n = u(x_j, t_n)$. Thus, u_j^0 is given by

$$u_j^0 = f(x_j). \tag{11}$$

We next obtain u_j^1, u_{j+1}^1, and u_{j-1}^1. Consider the second equation of Eq. (3). Using the *central difference* for the time derivative, we obtain from Eq. (3)

$$\left.\frac{\partial u(x,t)}{\partial t}\right|_{t=t_0,\, x=x_j} \approx \frac{u(x_j, t_{n+1}) - u(x_j, t_{n-1})}{2\Delta t} = \left.\frac{u_j^{n+1} - u_j^{n-1}}{2\Delta t}\right|_{n=0} = \frac{u_j^1 - u_j^{-1}}{2\Delta} = 0, \tag{12}$$

that is,

$$u_j^{-1} = u_j^1. \tag{13}$$

Equation (8) for $n = 0$ can be written as

$$u_j^1 = 2u_j^0 - u_j^{-1} + \frac{(\Delta t)^2}{(\Delta x)^2}\, a^2 \left(u_{j+1}^0 - 2u_j^0 + u_{j-1}^0\right). \tag{14}$$

Substituting Eq. (13) into Eq. (14), we obtain

$$2u_j^1 = 2u_j^0 + \frac{(\Delta t)^2}{(\Delta x)^2}\, a^2 \left(u_{j+1}^0 - 2u_j^0 + u_{j-1}^0\right), \tag{15}$$

which can recast into the form:

$$\boxed{u_j^1 = u_j^0 + \frac{(\Delta t)^2}{2(\Delta x)^2}\, a^2 \left(u_{j+1}^0 - 2u_j^0 + u_{j-1}^0\right).} \tag{16}$$

Thus, if the initial conditions

$$u_{j-1}^0 = f(x_{j-1}),\ u_j^0 = f(x_j),\ u_{j+1}^0 = f(x_{j+1}), \tag{17}$$

are given, we can obtain u_j^1 from Eq. (16). Furthermore, u_{j+1}^1 and u_{j-1}^1 can be written as

$$\left.\begin{aligned} u_{j+1}^1 &= u_{j+1}^0 + \frac{(\Delta t)^2}{2(\Delta x)^2}\, a^2 \left(u_{j+2}^0 - 2u_{j+1}^0 + u_j^0\right), \\ u_{j-1}^1 &= u_{j-1}^0 + \frac{(\Delta t)^2}{2(\Delta x)^2}\, a^2 \left(u_j^0 - 2u_{j-1}^0 + u_{j-2}^0\right). \end{aligned}\right\} \tag{18}$$

Thus, they can be obtained from the initial conditions:

$$u_{j-2}^0 = f(x_{j-2}),\ u_{j-1}^0 = f(x_{j-1}),\ u_j^0 = f(x_j),\ u_{j+1}^0 = f(x_{j+1}),\ u_{j+2}^0 = f(x_{j+2}), \tag{19}$$

We next obtain u_j^2 using Eq. (8). Equation (8) for $n = 1$ can be described as follow:

$$u_j^2 = 2u_j^1 - u_j^0 + \frac{(\Delta t)^2}{(\Delta x)^2}\, a^2 \left(u_{j+1}^1 - 2u_j^1 + u_{j-1}^1\right). \qquad (20)$$

where

$$\left.\begin{aligned} u_j^0 &= f(x_j), \\ u_j^1 &= u_j^0 + \frac{(\Delta t)^2}{2(\Delta x)^2}\, a^2 \left(u_{j+1}^0 - 2u_j^0 + u_{j-1}^0\right), \\ u_{j+1}^1 &= u_{j+1}^0 + \frac{(\Delta t)^2}{2(\Delta x)^2}\, a^2 \left(u_{j+2}^0 - 2u_{j+1}^0 + u_j^0\right), \\ u_{j-1}^1 &= u_{j-1}^0 + \frac{(\Delta t)^2}{2(\Delta x)^2}\, a^2 \left(u_j^0 - 2u_{j-1}^0 + u_{j-2}^0\right), \end{aligned}\right\} \qquad (21)$$

and $u_{j-2}^0,\ u_{j-1}^0,\ u_j^0,\ u_{j+1}^0$, and u_{j+2}^0 are given by Eq. (19). Thus we can obtain u_j^2 from Eq. (20). Similarly, we can sequentially obtain $u_j^3,\ u_j^4,\ u_j^5, \cdots$.

2.1.5 Boundary condition setting

Consider the difference equation (8) with N cells. The boundary conditions in Sec. 2.1.2 are described as follow:

- Dirichlet (fixed) boundary condition:

$$\left.\begin{aligned} u_1^n &= f(x_1), \\ u_N^n &= f(x_N). \end{aligned}\right\} \qquad (22)$$

- Periodic boundary condition:

$$\left.\begin{aligned} u_0^n &= u_N^n, \\ u_{N+1}^n &= u_1^n. \end{aligned}\right\} \qquad (23)$$

2.1.6 CNN circuit realization and difference equation approximation

We show the circuit realization of Eq. (8). Consider the resistor-coupled CNN shown in Fig. 1 [2] , where each cell consists of a *frequency-dependent negative resistor* (FNDR) with unit conductance ($G = 1$).[2] The dynamics of this circuit is given by

Dynamics of the resistor-coupled CNN in Fig. 1

$$\frac{d^2 v_j(t)}{dt^2} = \frac{1}{R}\left(v_{j+1}(t) - 2v_j(t) + v_{j-1}(t)\right). \qquad (24)$$

Let $v_j(t_n) = v_j^n$, where $t_n = t_0 + n\Delta t$. Using the second-order central difference for the time derivative, we obtain:

$$\left.\frac{d^2 v_j(t)}{dt^2}\right|_{t=t_n} \approx \frac{v_j(t_{n+1}) - 2v_j(t_n) + v_j(t_{n-1})}{(\Delta t)^2} = \frac{v_j^{n+1} - 2v_j^n + v_j^{n-1}}{(\Delta t)^2}, \qquad (25)$$

[2]The FNDR is a two-terminal linear element defined by $i = G(d^2 v/dt^2)$. It is a higher-order circuit element.

where $|\Delta t|$ is sufficiently small. Then, from Eq. (24), we get the following equation:

$$\begin{aligned} v_j^{n+1} &= 2v_j^n - v_j^{n-1} + \frac{(\Delta t)^2}{R}\left(v_{j+1}^n - 2v_j^n + v_{j-1}^n\right) \\ &= 2v_j^n - v_{j-1}^n + \frac{(\Delta t)^2}{(\Delta x)^2}\, a^2 \left(v_{j+1}^n - 2v_j^n + v_{j-1}^n\right), \end{aligned} \tag{26}$$

where we set $R = (\Delta x/a)^2$. It can be recast into the following difference equation:

Difference equation for Eq. (24)

$$v_j^{n+1} = 2v_j^n - v_{j-1}^n + \frac{(\Delta t)^2}{(\Delta x)^2}\, a^2 \left(v_{j+1}^n - 2v_j^n + v_{j-1}^n\right). \tag{27}$$

Thus, Eq. (27) is equivalent to Eq. (8), that is, they have the same solution. We call Eq. (27) as the second-order linear wave CNN Diff. Eq.

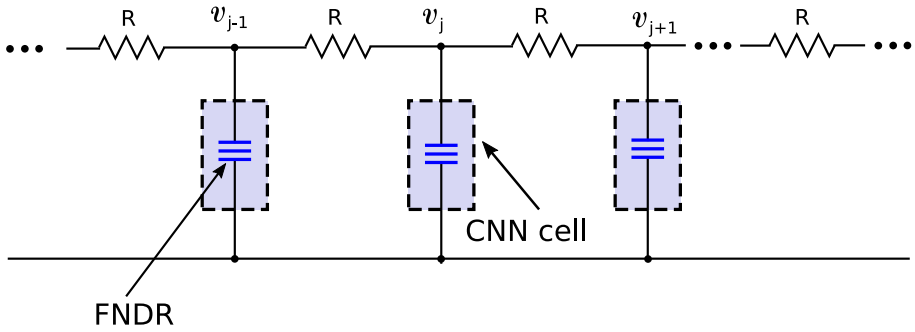

Figure 1: A CNN realization of Eq. (8) with linear resistor coupling between cells. The CNN cell consists of a FNDR (frequency-dependent negative resistor).

2.1.7 Computer simulations

Consider the second-order linear wave CNN Diff. Eq. (27) (equivalently, Eq. (8)) with $N = 200$ (cells). Assume that the boundary condition is given by the Dirichlet (fixed) boundary condition:

$$\left.\begin{aligned} u_1^n &= 0, \\ u_N^n &= 0. \end{aligned}\right\} \tag{28}$$

(A) pulse wave initial condition

Assume that the initial condition is given by the pulse with the height of 10:

$$u_j^0 = \begin{cases} 10 & (50 \le j \le 70), \\ 0 & (\text{otherwise}), \end{cases} \tag{29}$$

Note that the initial state, that is, the pulse is not continuously differentiable for all x. We show our computer simulations in Fig. 2, where the parameters for Eq. (27) are given by

$$a = 1,\ N = 200,\ \Delta t = 0.1,\ \Delta x = 0.1,\ 0 \le n \le 398. \tag{30}$$

Observe the following behavior of the solution:

1. A pulse splits into two pulses traveling with different direction.
2. When a pulse reaches the fixed boundary, it reflects back ($n = 61$). The reflected pulse is *inverted*.
3. After the interaction of the two pulses, they merge into one pulse ($n = 199$). It is the *reversing* pulse of the given initial pulse.
4. The reversed pulse splits into two pulses traveling with different direction. They merge into one pulse again ($n = 398$), which is identical to the initial condition.

The above procedure is repeated, again and again. It shows the *recurrence of the initial state*. Furthermore, the *total area of solutions* is constant, which is given by the product of the pulse-width and pulse-amplitude of the initial pulse, that is, $20 \times 10 = 200$. That is, Eq. (27) exhibits the *area-preserving* behavior. Thus, we conclude that the solutions of Eq. (27) can exhibit the following *soliton-like behavior*:

- A pulse splits into two pulses traveling with different direction. They move at constant speed.
- When a pulse interacts with another pulse, it emerges from the collision, and then it splits into two pulses.
- A solution returns exactly to its initial state (*recurrence of the initial state*).
- A solution exhibits the *area-preserving behavior*.

(B) two pulse wave initial condition

We next show the computer simulations when the two pulses are given as the initial state. Assume that the initial condition is given by

$$u_j^0 = \begin{cases} 10 & (50 \le j \le 70), \\ 10 & (150 \le j \le 170), \\ 0 & (\text{otherwise}). \end{cases} \tag{31}$$

Then we obtain the computer simulations in Fig. 3, where the parameters for Eq. (27) are given by

$$a = 1,\ N = 200,\ \Delta t = 0.1,\ \Delta x = 0.1,\ 0 \le n \le 796. \tag{32}$$

Observe that the solution exhibits the same behavior as the case of the one pulse. That is, the two initial pulses are split into four pulses, and the solution of Eq. (8) eventually returns to the initial state after the interaction of the pulses ($n = 398,\ 796$). Furthermore, the *total pulse area* is constant, which is equal to $20 \times 10 + 20 \times 10 = 400$.

(C) sine wave initial condition

Assume next that the initial condition is given by the sine wave:

$$u_j^0 = \sin\left[2\pi\left(\frac{j-1}{N}\right)\right], \tag{33}$$

where $j = 1, 2, \cdots, 200$, and the boundary condition is given by Eq. (28). We show our computer simulations in Fig. 4, where the parameters for Eq. (27) are given by

$$a = 1,\ N = 200,\ \Delta t = 0.1,\ \Delta x = 0.1,\ 0 \le n \le 400. \tag{34}$$

Observe that the solution represents the vibration of a string. In our computer simulations, the initial wave dose not evolve into a solitary-type wave.

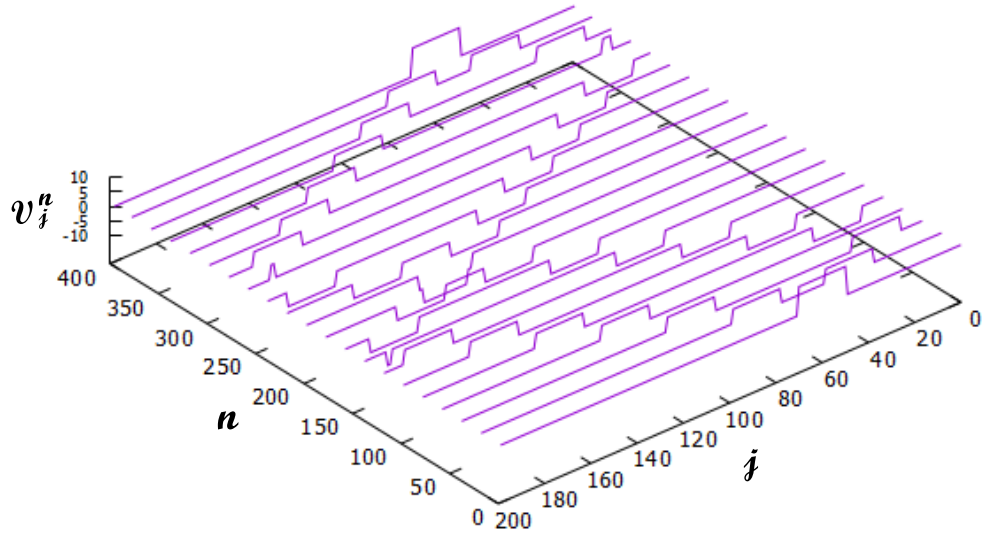

(a)

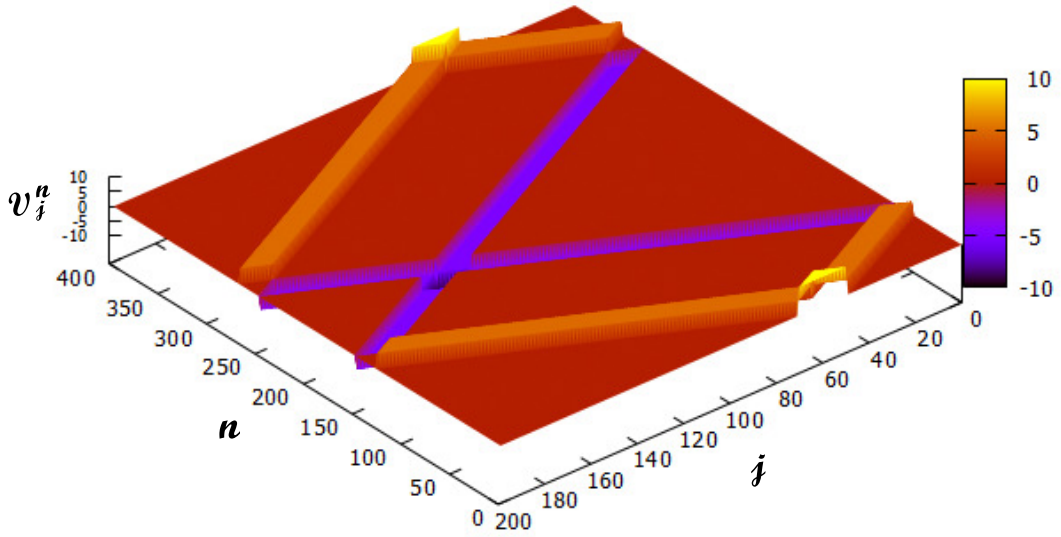

(b)

Figure 2: Three-dimensional plots of soliton-like waves in the second-order linear wave CNN Diff. Eq. (27). Two different plots of the soliton-like waves are shown. The initial condition is given by the pulse with the height of 10. The boundary condition is given by the Dirichlet (fixed) boundary condition. Observe that a pulse splits into two pulses traveling with different direction. They move at constant speed. When a pulse reaches the fixed boundary, it reflects back ($n = 61$). The reflected pulse is inverted. After the interaction of the two pulses, they merge into one pulse ($n = 199$). It is the reversing pulse of the given initial pulse. The above reversed pulse splits into two pulses traveling with different direction. They merge into one pulse again ($n = 398$), which is identical to the initial condition. That is, the solution returns exactly to its initial state. Furthermore, it exhibits the area-preserving behavior.

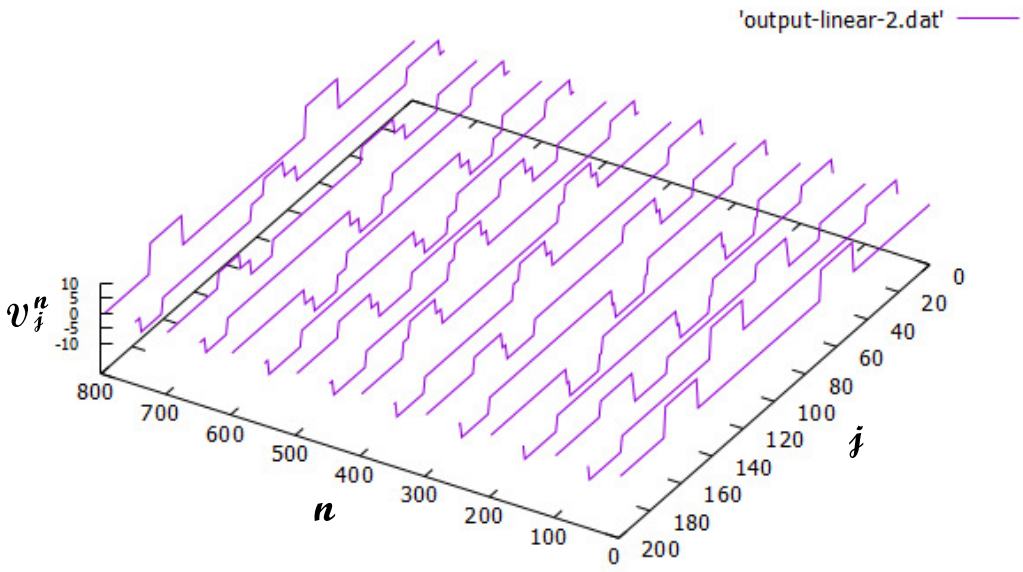

(a)

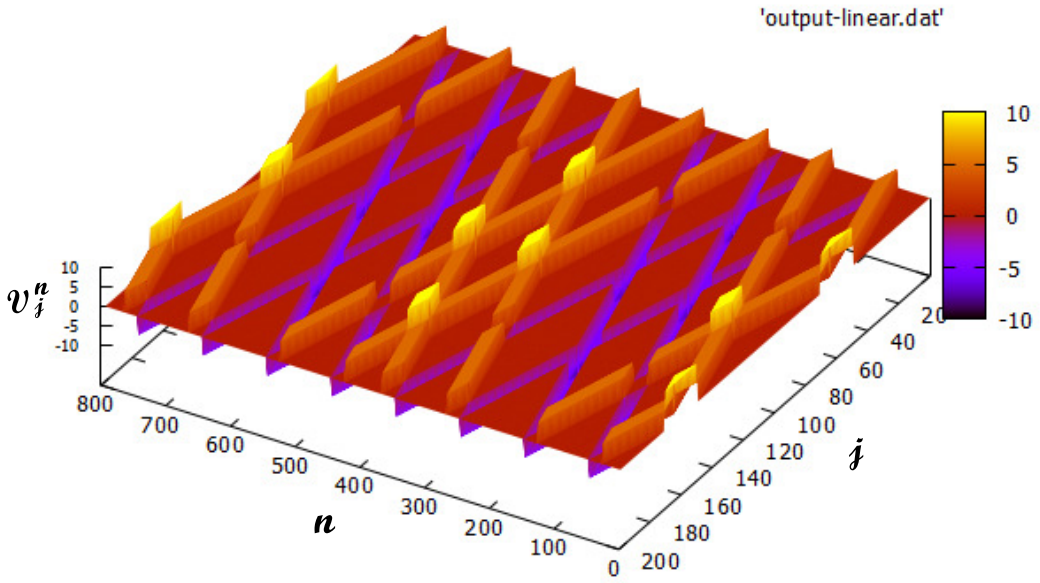

(b)

Figure 3: Three-dimensional plots of soliton-like waves in the second-order linear wave CNN Diff. Eq. (27). Two different plots of the soliton-like waves are shown. The initial condition is given by the two pulse with the height of 10. The boundary condition is given by the Dirichlet (fixed) boundary condition. The solution returns exactly to its initial state (two pulses) at $n = 398,\ 796$.

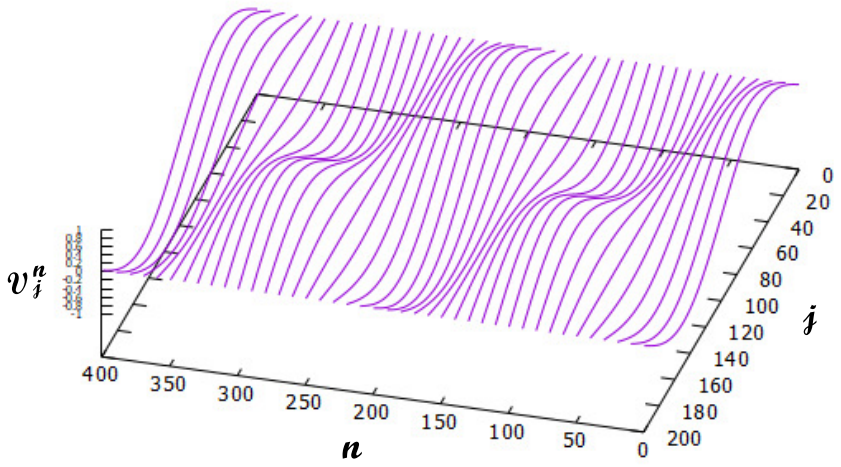

(a)

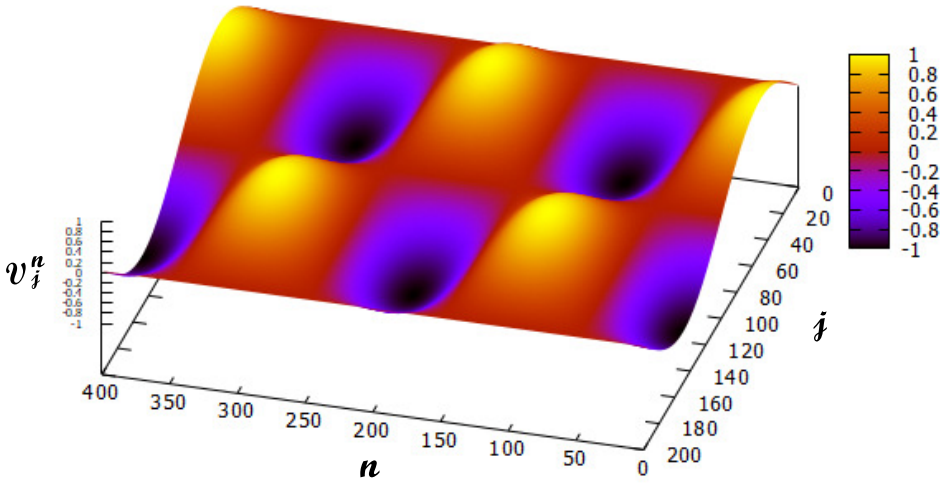

(b)

Figure 4: Three-dimensional plots of the solutions in the second-order linear wave CNN Diff. Eq. (27). Two different plots of the waves are shown. The initial condition is given by the sine wave. The boundary condition is given by the Dirichlet (fixed) boundary condition. The solution represents the vibration of a string. In this case, the initial wave dose not evolve into a solitary-type wave.

2.2 First-order linear wave equation

Consider the second-order wave equation

$$\frac{\partial^2 w(x,t)}{\partial t^2} = a^2 \frac{\partial^2 w(x,t)}{\partial x^2}, \tag{35}$$

where $w(x,t)$ is the amplitude of the wave. Then Eq. (36) can be written as

$$\left[\frac{\partial}{\partial t} + a\frac{\partial}{\partial x}\right]\left[\frac{\partial}{\partial t} - a\frac{\partial}{\partial x}\right] w(x,t) = 0. \tag{36}$$

Define

$$u(x,t) \stackrel{\text{def}}{=} \left[\frac{\partial}{\partial t} - a\frac{\partial}{\partial x}\right] w(x,t). \tag{37}$$

Then, Eq. (36) can be recast into

$$\left[\frac{\partial}{\partial t} + a\frac{\partial}{\partial x}\right] u(x,t) = 0. \tag{38}$$

Similarly, define

$$u(x,t) \stackrel{\text{def}}{=} \left[\frac{\partial}{\partial t} + a\frac{\partial}{\partial x}\right] w(x,t). \tag{39}$$

Then, Eq. (36) can be recast into

$$\left[\frac{\partial}{\partial t} - a\frac{\partial}{\partial x}\right] u(x,t) = 0. \tag{40}$$

Thus, we study next the *first-order* wave equations defined by

$$\left.\begin{array}{ll} \text{(a)} & \left[\dfrac{\partial}{\partial t} + a\dfrac{\partial}{\partial x}\right] u(x,t) = 0, \\ \text{(b)} & \left[\dfrac{\partial}{\partial t} - a\dfrac{\partial}{\partial x}\right] u(x,t) = 0, \end{array}\right\} \tag{41}$$

or equivalently

First-order linear wave equations

$$\left.\begin{array}{ll} \text{(a)} & \dfrac{\partial u(x,t)}{\partial t} + a\dfrac{\partial u(x,t)}{\partial x} = 0, \\ \text{(b)} & \dfrac{\partial u(x,t)}{\partial t} - a\dfrac{\partial u(x,t)}{\partial x} = 0. \end{array}\right\} \tag{42}$$

The general solutions of Eq. (42)(a) and (b) are given by

$$\left.\begin{array}{ll} \text{(a)} & u(x,t) = \xi(x-at), \\ \text{(b)} & u(x,t) = \eta(x+at), \end{array}\right\} \tag{43}$$

respectively, where $\xi(x)$ and $\eta(x)$ are arbitrary functions that are continuously differentiable for all x.

2.2.1 Approximating the first-order linear wave equation

We approximate Eq. (42) by using the central difference scheme. Let us define u_j^n by

$$u_j^n \stackrel{\text{def}}{=} u(x_j, t_n), \tag{44}$$

where $x_j = x_0 + j\Delta x$ and $t_n = t_0 + n\Delta t$ (x_0, t_0, Δx, and Δt are some constants, and j and n are integers). Using the *central difference* for the space and time derivatives, we obtain:

$$\left.\begin{aligned} \left.\frac{\partial u(x,t)}{\partial t}\right|_{t=t_n,\, x=x_j} &\approx \frac{u(x_j, t_{n+1}) - u(x_j, t_{n-1})}{(2\Delta t)} &&= \frac{u_j^{n+1} - u_j^{n-1}}{(2\Delta t)}, \\ \left.\frac{\partial u(x,t)}{\partial x}\right|_{t=t_n,\, x=x_j} &\approx \frac{u(x_{j+1}, t_n) - u(x_{j-1}, t_n)}{(2\Delta x)} &&= \frac{u_{j+1}^n - u_{j-1}^n}{(2\Delta x)}, \end{aligned}\right\} \tag{45}$$

where $|\Delta x|$ and $|\Delta t|$ are sufficiently small. Then, Eq. (42) can be approximated by the following difference equations:

$$\left.\begin{aligned} &\text{(a)} \quad \frac{u_j^{n+1} - u_j^{n-1}}{2\Delta t} + a\frac{u_{j+1}^n - u_{j-1}^n}{2\Delta x} = 0, \\ &\text{(b)} \quad \frac{u_j^{n+1} - u_j^{n-1}}{2\Delta t} - a\frac{u_{j+1}^n - u_{j-1}^n}{2\Delta x} = 0. \end{aligned}\right\} \tag{46}$$

They can be recast into the form

Difference equations for Eq. (42)

$$\left.\begin{aligned} &\text{(a)} \quad u_j^{n+1} = u_j^{n-1} - \frac{\Delta t}{\Delta x}\, a\,(u_{j+1}^n - u_{j-1}^n), \\ &\text{(b)} \quad u_j^{n+1} = u_j^{n-1} + \frac{\Delta t}{\Delta x}\, a\,(u_{j+1}^n - u_{j-1}^n). \end{aligned}\right\} \tag{47}$$

2.2.2 Boundary condition setting

Consider the difference equation (47) with N cells. The boundary conditions in Sec. 2.1.2 are described as follow:

- Dirichlet (fixed) boundary condition:

$$\left.\begin{aligned} u_1^n &= f(x_1), \\ u_N^n &= f(x_N). \end{aligned}\right\} \tag{48}$$

- Periodic boundary condition:

$$\left.\begin{aligned} u_0^n &= u_N^n \\ u_{N+1}^n &= u_1^n \end{aligned}\right\} \tag{49}$$

2.2.3 CNN circuit realization

We show the circuit realization of Eq. (47). Consider the resistor-coupled CNN shown in Fig. 5, where each cell consists of a capacitor $C$and a voltage-controlled current source I_j. The dynamics of this circuit is given

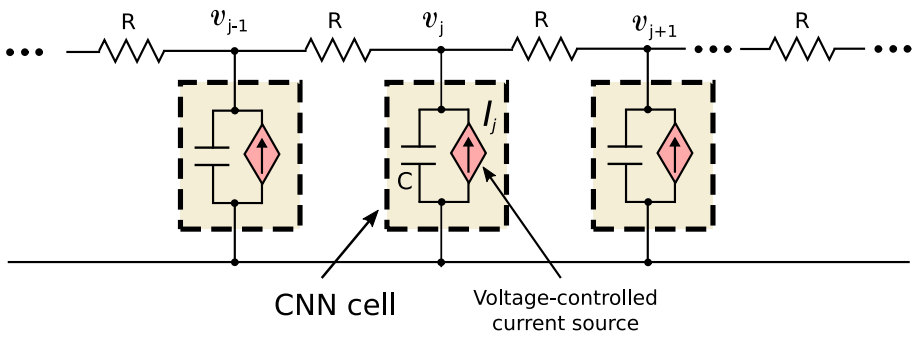

Figure 5: A CNN realization of Eq. (47) with linear resistor coupling between cells. The CNN cell consists of a capacitor C and a voltage-controlled current source I_j, where $C = 1$ and $I_j = 2(v_j - v_{j-1})/R$.

by

$$\left.\begin{aligned} C\frac{dv_j(t)}{dt} &= \frac{v_{j+1}(t) - 2v_j(t) + v_{j-1}(t)}{R} + I_j \\ &= \frac{v_{j+1}(t) - 2v_j(t) + v_{j-1}(t)}{R} + \frac{2(v_j(t) - v_{j-1}(t))}{R} \\ &= \frac{v_{j+1}(t) - v_{j-1}(t)}{R} \end{aligned}\right\} \tag{50}$$

where $C = 1$ and $I_j = 2(v_j - v_{j-1})/R$. Thus, we can obtain the following equation:

Dynamics of the resistor-coupled CNN in Fig. 5

$$\frac{dv_j(t)}{dt} = \frac{v_{j+1}(t) - v_{j-1}(t)}{R} \tag{51}$$

Using the *central difference* for the time derivative, we obtain:

$$\left.\frac{\partial v_j(t)}{\partial t}\right|_{t=t_n} \approx \frac{v_j(t_{n+1}) - v_j(t_{n-1})}{2\Delta t} = \frac{v_j^{n+1} - v_j^{n-1}}{2\Delta t}, \tag{52}$$

where $v_j^n = v_j(t_n)$, $t_n = t_0 + n\Delta t$, and $|\Delta t|$ is sufficiently small. Then, we can approximate Eq. (51) by the following difference equation:

$$\frac{v_j^{n+1} - v_j^{n-1}}{2\Delta t} = \frac{v_{j+1}^n - v_{j-1}^n}{R}, \tag{53}$$

It can be recast into the form

Difference equations for Eq. (51)

$$\left.\begin{aligned} &\text{(a)} \quad v_j^{n+1} = v_j^{n-1} - \frac{\Delta t}{\Delta x}\, a\,(v_{j+1}^n - u_{j-1}^n) \qquad \text{for} \quad R = -2\Delta x, \\ &\text{(b)} \quad v_j^{n+1} = v_j^{n-1} + \frac{\Delta t}{\Delta x} a\,(v_{j+1}^n - u_{j-1}^n) \qquad \text{for} \quad R = 2\Delta x. \end{aligned}\right\} \tag{54}$$

Thus, Eq. (54) is equivalent to Eq. (47), that is, they have the same solution. We call Eq. (54) as the first-order linear wave CNN Diff. Eqs.

2.2.4 Computer simulations

Consider the first-order linear wave CNN Diff. Eq. (54)(a). We study the behavior of its solutions for the two kinds of initial conditions.

- Case 1. Assume that the initial condition is given by the unit step function:

$$v_j^0 = \begin{cases} 0 & (j \geq 100), \\ 1 & (\text{otherwise}), \end{cases} \tag{55}$$

and the boundary condition is given by the Dirichlet (fixed) boundary condition:

$$\left.\begin{array}{rcl} v_1^n & = & 1, \\ v_N^n & = & 0. \end{array}\right\} \tag{56}$$

where $N = 250$ (cells). We show our computer simulations in Fig. 6, where the parameters for Eq. (54)(a) are given by

$$a = 0.2,\ N = 200,\ \Delta t = 0.05,\ \Delta x = 0.3,\ 0 \leq n \leq 500. \tag{57}$$

Observe that the initial wave evolves into a train of *solitary-like* waves. They are generated in the neighborhood of the discontinuity point of the initial wave. These solitary-like waves move to the right at a constant speed. Note that the initial state (condition), that is, the unit step function is not continuously differentiable for all x.[3]

- Case 2. The initial condition is given by the cos function:

$$v_j^0 = \cos\left[2\pi\left(\frac{j}{N-1}\right)\right], \tag{58}$$

and the boundary condition is given by the periodic boundary condition:

$$\left.\begin{array}{rcl} v_0^n & = & v_N^n, \\ v_{N+1}^n & = & v_1^n, \end{array}\right\} \tag{59}$$

where $N = 256$ (cells). We show our computer simulations in Fig. 7, where the parameters for Eq. (54)(a) are given by

$$a = 0.2,\ N = 256,\ \Delta t = 0.05,\ \Delta x = 0.3,\ 0 \leq n \leq 3000. \tag{60}$$

Observe that the initial sine wave moves at a constant speed without distortion. This behavior is quite different from that of Case 1.

[3]The general solutions of Eq. (42) are continuously differentiable for all x.

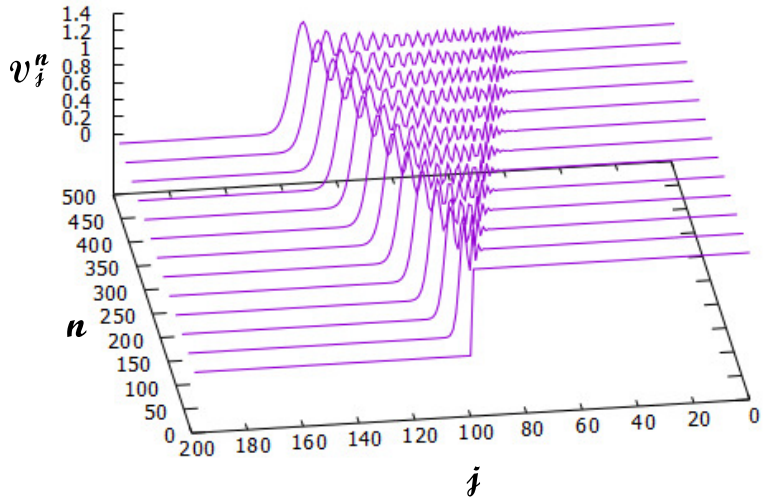

(a)

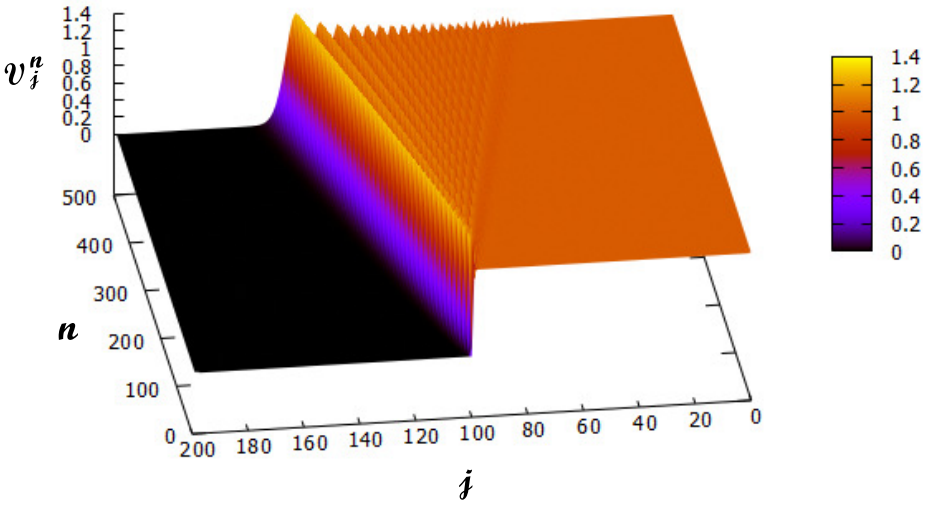

(b)

Figure 6: Three-dimensional plots of soliton waves in the first-order linear wave CNN Diff. Eq. (54). Two different plots of the soliton-like waves are shown. The initial condition is given by the unit step function and the boundary condition is given by the Dirichlet (fixed) boundary condition. Observe that the initial wave evolves into a train of solitary-like waves.

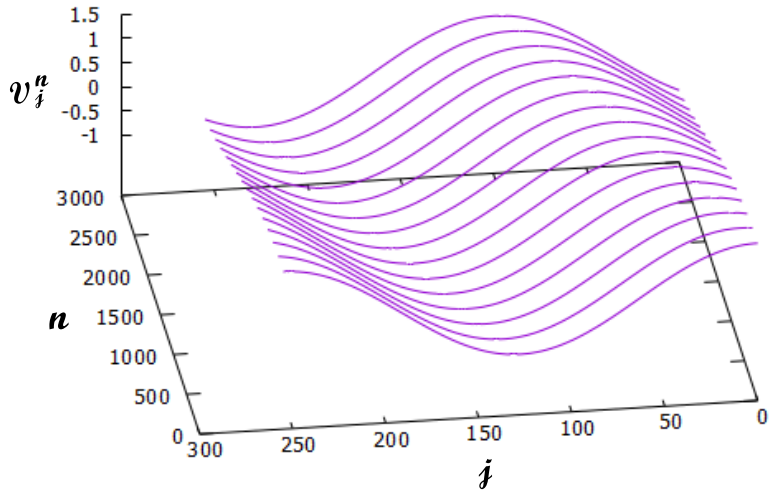

(a)

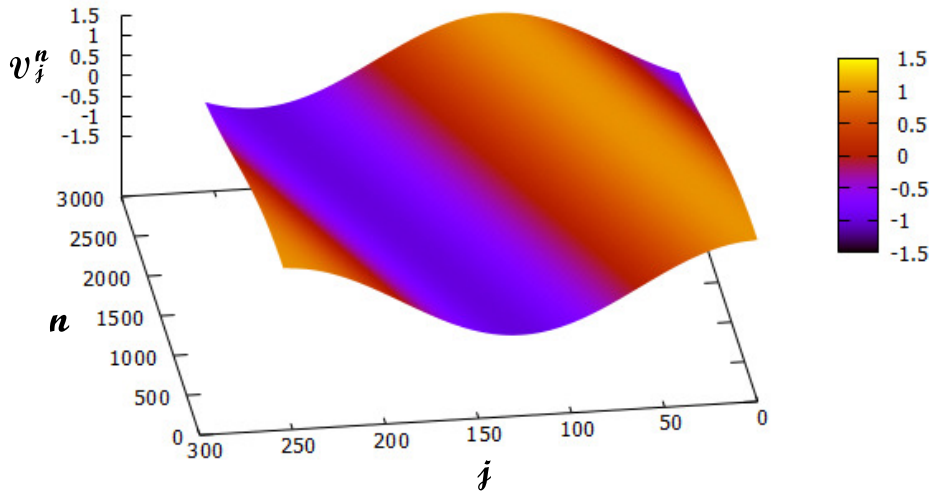

(b)

Figure 7: Three-dimensional plots of soliton waves in the first-order linear wave CNN Diff. Eq. (54). Two different plots of the waves are shown. The initial condition is given by the cos function and the boundary condition is given by the periodic boundary condition. Observe that the initial sine wave moves at a constant speed without distortion.

2.3 First-order nonlinear wave equation

The simplest first-order nonlinear wave (or kinematic wave) equation is

First-order nonlinear wave equation

$$\frac{\partial u(x,t)}{\partial t} + c(u)\frac{\partial u(x,t)}{\partial x} = 0. \tag{61}$$

where $u(x,t)$ is the amplitude of the wave at position x and time t, and $c(u)$ is a given function of u. This nonlinear equation describes the propagation of a nonlinear wave in the negative direction of the x-axis with velocity $c(u)$.

2.3.1 Difference equation approximation

We approximate Eq. (61) by using the central difference scheme. Let us define u_j^n by

$$u_j^n \stackrel{\text{def}}{=} u(x_j, t_n), \tag{62}$$

where $x_j = x_0 + j\Delta x$ and $t_n = t_0 + n\Delta t$ (x_0, t_0, Δx, and Δt are some constants), and j and n are integers). Using the *central difference* for the space and time derivatives, we obtain

$$\left.\begin{aligned} \left.\frac{\partial u(x,t)}{\partial t}\right|_{t=t_n,\, x=x_j} &\approx \frac{u(x_j,t_{n+1}) - u(x_j,t_{n-1})}{2\Delta t} = \frac{u_j^{n+1} - u_j^{n-1}}{2\Delta t}, \\ \left.\frac{\partial u(x,t)}{\partial x}\right|_{t=t_n,\, x=x_j} &\approx \frac{u(x_{j+1},t_n) - u(x_{j-1},t_n)}{2\Delta x} = \frac{u_{j+1}^{n} - u_{j-1}^{n}}{2\Delta x}, \end{aligned}\right\} \tag{63}$$

where $|\Delta x|$ and $|\Delta t|$ are sufficiently small. Then, we can approximate Eq. (61) by the following difference equation:

Difference equation for Eq. (61)

$$u_j^{n+1} = u_j^{n-1} - \frac{\Delta t}{\Delta x}\, c(u_j^n)\,(u_{j+1}^n - u_{j-1}^n). \tag{64}$$

2.3.2 CNN circuit realization and difference equation approximation

We show the circuit realization of Eq. (64). Consider the CNN cell in Fig. 5. If we replace voltage-controlled current source I_j in Fig. 5 with

$$I_j = \frac{2(v_j - v_{j-1})}{R} + \frac{(v_{j+1} - v_{j-1})\delta(v_j)}{R}, \tag{65}$$

then the dynamics of the circuit in Fig. 5 is given by

$$\begin{aligned} C\frac{dv_j(t)}{dt} &= \frac{v_{j+1}(t) - 2v_j(t) + v_{j-1}(t)}{R} + I_j \\ &= \frac{v_{j+1}(t) - 2v_j(t) + v_{j-1}(t)}{R} + \frac{2(v_j(t) - v_{j-1}(t))}{R} + \frac{(v_{j+1}(t) - v_{j-1}(t))\delta(v_j(t))}{R} \\ &= -\frac{(1 + \delta(v_j(t)))(v_j(t) - v_{j-1}(t))}{R} = -\frac{c(v_j(t))(v_{j+1}(t) - v_{j-1}(t))}{R}, \end{aligned} \tag{66}$$

where $\delta(v_j)$ is a function of v_j and $c(v_j) \stackrel{\text{def}}{=} 1 + \delta(v_j)$. Thus, we can obtain the following equation:

Dynamics of the resistor-coupled CNN in Fig. 5

$$C\frac{dv_j(t)}{dt} = -\frac{c\big(v_j(t)\big)\big(v_{j+1}(t) - v_{j-1}(t)\big)}{R}. \tag{67}$$

Using the *central difference* for the time derivative, we obtain

$$\left.\frac{dv_j(t)}{dt}\right|_{t=t_n} \approx \frac{v_j(t_{n+1}) - v_j(t_{n-1})}{2\Delta t} = \frac{v_j^{n+1} - v_j^{n-1}}{2\Delta t} \tag{68}$$

Then, we can approximate Eq. (67) by the following difference equation:

$$C\left(\frac{v_j^{n+1} - v_j^{n-1}}{2\Delta t}\right) = -\frac{c(v_j^n)\,(v_{j+1}^n - v_{j-1}^n)}{R}, \tag{69}$$

where $v_j^n = v_j(t_n)$, $t_n = t_0 + n\Delta t$, and $|\Delta t| \ll 1$. If we assume that $C = 1$ and $R = 2\Delta x$, then we obtain

Difference equation for Eq. (67)

$$v_j^{n+1} = v_j^{n-1} - \frac{\Delta t}{\Delta x}\, c(v_j^n)\,(v_{j+1}^n - v_{j-1}^n), \tag{70}$$

Thus, Eq. (70) is equivalent to Eq. (64), that is, they have the same solution. We call Eq. (70) as the first-order nonlinear wave CNN Diff. Eq.

2.3.3 Boundary condition setting

Consider the discrete wave equation (47) with N cells. The boundary conditions in Sec. 2.1.2 are described as follow:

- Dirichlet (fixed) boundary condition:

$$\left.\begin{aligned} u_1^n &= f(x_1), \\ u_N^n &= f(x_N). \end{aligned}\right\} \tag{71}$$

- Periodic boundary condition:

$$\left.\begin{aligned} u_0^n &= u_N^n, \\ u_{N+1}^n &= u_1^n. \end{aligned}\right\} \tag{72}$$

2.3.4 Computer simulations

Consider the first-order linear wave CNN Diff. Eq. (70) with $N = 256$ (cells). Assume that the initial condition is given by the sine wave:

$$v_j^0 = \sin\left[2\pi\left(\frac{j}{N-1}\right)\right], \tag{73}$$

and the boundary condition is given by the Dirichlet (fixed) boundary condition:

$$\left.\begin{aligned} v_1^n &= 0, \\ v_N^n &= 0, \end{aligned}\right\} \tag{74}$$

where $j = 1, 2, \cdots, 256$. We show our computer simulations in Fig. 7, where the parameters for Eq. (70) are given by

$$a = 0.2,\ N = 256,\ \Delta t = 0.05,\ \Delta x = 0.3,\ 0 \leq n \leq 1250. \tag{75}$$

Observe that the shape of the initial curve is distorted continuously with increasing time, if the initial condition is given by the *sin wave*. That is, the wave gets progressively steeper until the wave overtops, and ultimately the waveform breaks down (a floating point overflow occurs in our computer simulations). It is due to the reason that the solution becomes multiple-valued for t.

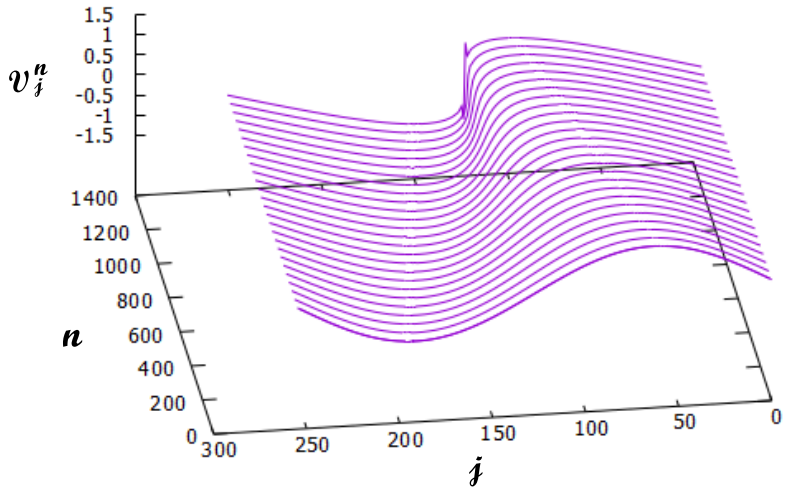

(a)

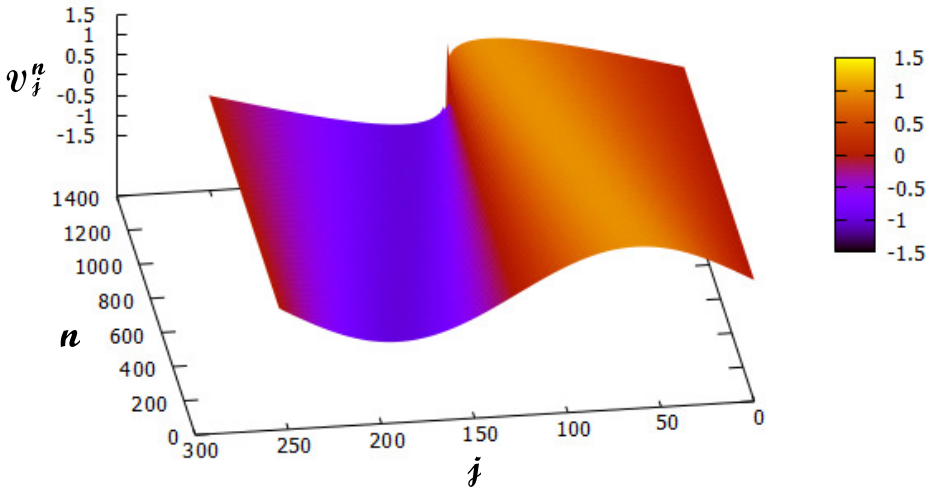

(b)

Figure 8: Three-dimensional plots of soliton waves in the first-order nonlinear wave CNN Diff. Eq. (70). Two different plots of the waves are shown. The initial condition is given by the sine wave and the boundary condition is given by the Dirichlet (fixed) boundary condition. Observe that the shape of the initial curve is distorted continuously with increasing time, and the wave gets progressively steeper until the wave overtops.

3 Korteweg-de Vries Equation

The Korteweg-de Vries (KdV) equation is one of the most well known of all nonlinear partial differential equations. It was proposed by D. Korteweg and G. de Vries [6] to describe weakly nonlinear shallow water waves:

$$\frac{\partial u(x,t)}{\partial t} + a\,u(x,t)\frac{\partial u(x,t)}{\partial x} + b\frac{\partial^3 u(x,t)}{\partial x^3} = 0. \tag{76}$$

where a and b are constants.[4]

3.1 Difference equation approximation

We approximate Eq. (76) by using the central difference scheme. Let us define u_j^n by

$$u_j^n \stackrel{\text{def}}{=} u(x_j, t_n) \tag{77}$$

where $x_j = x_0 + j\Delta x$ and $t_n = t_0 + n\Delta t$ (x_0, t_0, Δx, and Δt are some constants, and j and n are integers).

Using the *finite difference approximations* for the time and space derivatives, we obtain:

$$\left.\begin{aligned} \left.\frac{\partial u(x,t)}{\partial t}\right|_{t=t_n,\,x=x_j} &\approx \frac{u_j^{n+1} - u_j^{n-1}}{2\Delta t}, \\ \left.\frac{\partial u(x,t)}{\partial x}\right|_{t=t_n,\,x=x_j} &\approx \frac{u_{j+1}^{n} - u_{j-1}^{n}}{2\Delta x}, \\ \left.\frac{\partial^3 u(x,t)}{\partial x^3}\right|_{t=t_n,\,x=x_j} &\approx \frac{u_{j+2}^{n} - 2u_{j+1}^{n} + 2u_{j-1}^{n} - u_{j-2}^{n}}{2(\Delta x)^3}, \end{aligned}\right\} \tag{78}$$

where $|\Delta t|$ and $|\Delta x|$ are sufficiently small. Substituting Eq. (78) into Eq. (76), we obtain

$$\frac{u_j^{n+1} - u_j^{n-1}}{2\Delta t} + a u_j^n \left(\frac{u_{j+1}^n - u_{j-1}^n}{2\Delta x}\right) + b\frac{u_{j+2}^n - 2u_{j+1}^n + 2u_{j-1}^n - u_{j-2}^n}{2(\Delta x)^3} = 0, \tag{79}$$

or equivalently

$$u_j^{n+1} = u_j^{n-1} - \left(\frac{a\Delta t}{\Delta x}\right) u_j^n\,(u_{j+1}^n - u_{j-1}^n) - \left(\frac{b\Delta t}{\Delta x^3}\right)(u_{j+2}^n - 2u_{j+1}^n + 2u_{j-1}^n - u_{j-2}^n). \tag{80}$$

3.2 Boundary condition setting

Consider the discrete wave equation (80) with N cells. The boundary conditions in Sec. 2.1.2 are described as follow:

- Dirichlet (fixed) boundary condition:

$$\left.\begin{aligned} u_1^n &= u_2^n &&= f(x_1), \\ u_N^n &= u_{N-1}^n &&= f(x_N). \end{aligned}\right\} \tag{81}$$

- Periodic boundary condition:

$$\left.\begin{aligned} u_0^n &= u_N^n, \\ u_{-1}^n &= u_{N-1}^n, \\ u_{N+1}^n &= u_1^n, \\ u_{N+2}^n &= u_2^n. \end{aligned}\right\} \tag{82}$$

[4] In [1], the parameters a and b are set to 1 and $(0.022)^2$, respectively.

3.3 CNN circuit realization and difference equation approximation

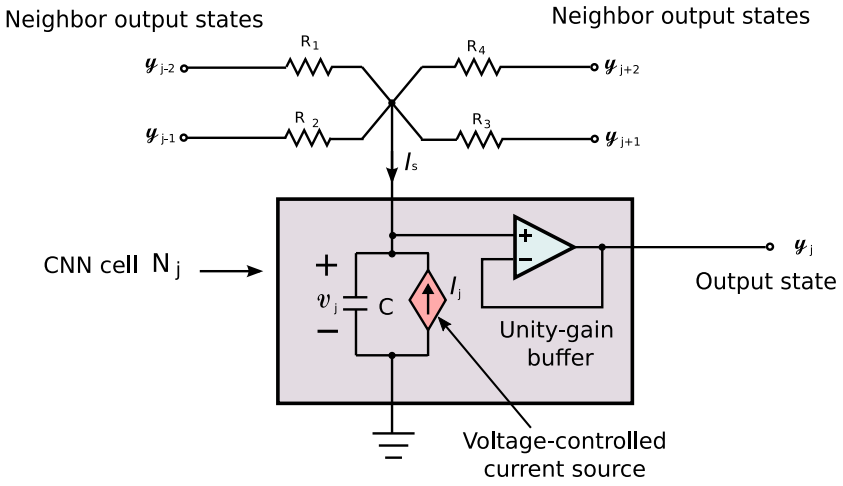

Figure 9: A CNN realization of Eq. (80). The CNN cell N_j consists of three elements, that is, a capacitor C, a voltage-controlled current source I_j, and a unity-gain buffer. Here, $C = 1$, $I_j = -\left(\frac{a}{2\Delta x}\right) y_j^n \, (y_{j+1}^n - y_{j-1}^n)$, and $v_j = y_j$. Each CNN cell are connected to four neighbor cells using the four resistors $R_i \, (i = 1, 2, 3, 4)$. A unity gain buffer is an op-amp circuit which has a voltage gain of 1.

We show the circuit realization of Eq. (80). Consider the CNN cell model shown in Fig. 9, where the cell consists of a capacitor C, a voltage-controlled current source I_j, and a unity gain buffer. The dynamics of this circuit is given by

$$\begin{aligned} C\frac{dv_j(t)}{dt} &= I_j + I_s \\ &= -\left(\frac{a}{2\Delta x}\right) y_j \, (y_{j+1} - y_{j-1}) + \frac{y_{j-2} - y_j}{R_1} + \frac{y_{j-1} - y_j}{R_2} + \frac{y_{j+1} - y_j}{R_3} + \frac{y_{j+2} - y_j}{R_4} \end{aligned} \tag{83}$$

where

$$\begin{aligned} I_j &= -\left(\frac{a}{2\Delta x}\right) y_j^n \, (y_{j+1} - y_{j-1}) \\ I_s &= \frac{y_{j-2} - y_j}{R_1} + \frac{y_{j-1} - y_j}{R_2} + \frac{y_{j+1} - y_j}{R_3} + \frac{y_{j+2} - y_j}{R_4} \end{aligned} \tag{84}$$

If we set

$$C = 1, \; R_1 = -\frac{2\Delta x^3}{b}, \; R_2 = \frac{\Delta x^3}{b}, \; R_3 = -\frac{\Delta x^3}{b}, \; R_4 = \frac{2\Delta x^3}{b}, \tag{85}$$

then we obtain

$$\begin{aligned} \frac{dv_j}{dt} &= -\left(\frac{a}{2\Delta x}\right) y_j^n \, (y_{j+1}^n - y_{j-1}^n) + \left(\frac{b}{2\Delta x^3}\right) \left[-(y_{j-2}^n - v_j^n) + 2(y_{j-1}^n - v_j^n) - 2(y_{j+1}^n - v_j^n) + (y_{j+2}^n - v_j^n)\right] \\ &= -\left(\frac{a}{2\Delta x}\right) y_j^n \, (y_{j+1}^n - y_{j-1}^n) - \left(\frac{b}{2\Delta x^3}\right) (y_{j+2}^n - 2y_{j+1}^n + 2y_{j-1}^n - v_{j-2}^n), \end{aligned} \tag{86}$$

where $v_j = y_j$. Let $v_j(t_n) = v_j^n$, where $t_n = t_0 + n\Delta t$. Using the *central difference* for the time derivative, we obtain:

$$\left.\frac{\partial v_j(t)}{\partial t}\right|_{t=t_n} \approx \frac{v_j^{n+1} - v_j^{n-1}}{2\Delta t}, \tag{87}$$

where Δt is sufficiently small. Then, from Eq. (86), we get the difference equation:

$$v_j^{n+1} = v_j^{n-1} - \left(\frac{a\Delta t}{\Delta x}\right) v_j^n \left(v_{j+1}^n - v_{j-1}^n\right) - \left(\frac{b\Delta t}{\Delta x^3}\right)\left(v_{j+2}^n - 2v_{j+1}^n + 2v_{j-1}^n - v_{j-2}^n\right), \tag{88}$$

where we replaced y_j with v_j, since $v_j = y_j$. Thus, Eq. (88) is equivalent to Eq. (80), that is, they have the same solution. We call Eq. (88) as the Korteweg-de Vries (KdV) CNN Diff. Eq.

3.4 Memristor CNN cell model

Consider next the CNN cell model shown in Fig. 10, where we replaced the voltage-controlled current source in Fig. 9 with the coupled extended memristor. The dynamics of this circuit is given by

$$\begin{aligned} C\frac{dv_j}{dt} &= I_s + i_M \\ &= -\left(\frac{a}{2\Delta x}\right)\left(y_{j+1} - y_{j-1}\right) W(\varphi_j)\, v_M + \frac{y_{j-2} - y_j}{R_1} + \frac{y_{j-1} - y_j}{R_2} + \frac{y_{j+1} - y_j}{R_3} + \frac{y_{j+2} - y_j}{R_4}, \\ \frac{d\varphi_j}{dt} &= v_j, \end{aligned} \tag{89}$$

where

$$\begin{aligned} i_M &= -\left(\frac{a}{2\Delta x}\right)\left(y_{j+1} - y_{j-1}\right) W(\varphi_j)\, v_M, \\ v_M &= v_j = y_j, \\ I_s &= \frac{y_{j-2} - y_j}{R_1} + \frac{y_{j-1} - y_j}{R_2} + \frac{y_{j+1} - y_j}{R_3} + \frac{y_{j+2} - y_j}{R_4}, \end{aligned} \tag{90}$$

The v-i characteristic of the coupled extended memristor is given by

$$i_M = -\left(\frac{a}{2\Delta x}\right)\left(y_{j+1} - y_{j-1}\right) W(\varphi_j)\, v_M, \tag{91}$$

where φ_j is the flux of the coupled extended memristor and $W(\varphi_j)$ is a scalar function of φ_j ($\frac{d\varphi_j}{dt} = v_M$).

Using the *central difference* for the time derivative, we get the difference equation:

$$\left.\begin{aligned} v_j^{n+1} &= v_j^{n-1} - \left(\frac{a\Delta t}{\Delta x}\right)\left(v_{j+1}^n - v_{j-1}^n\right) W(\varphi_j^n)\, v_j^n - \left(\frac{b\Delta t}{\Delta x^3}\right)\left(v_{j+2}^n - 2v_{j+1}^n + 2v_{j-1}^n - v_{j-2}^n\right), \\ \varphi_j^{n+1} &= \varphi_j^{n-1} + 2(\Delta t)\, v_j^n, \end{aligned}\right\} \tag{92}$$

where $v_j(t_n) = v_j^n$, $\varphi_j(t_n) = \varphi_j^n$, $t_n = t_0 + n\Delta t$, and the circuit parameters are given by

$$C = 1,\ R_1 = -\frac{2\Delta x^3}{b},\ R_2 = \frac{\Delta x^3}{b},\ R_3 = -\frac{\Delta x^3}{b},\ R_4 = \frac{2\Delta x^3}{b}. \tag{93}$$

We call Eq. (92) as the Korteweg-de Vries (KdV) memristor CNN Diff. Eq.

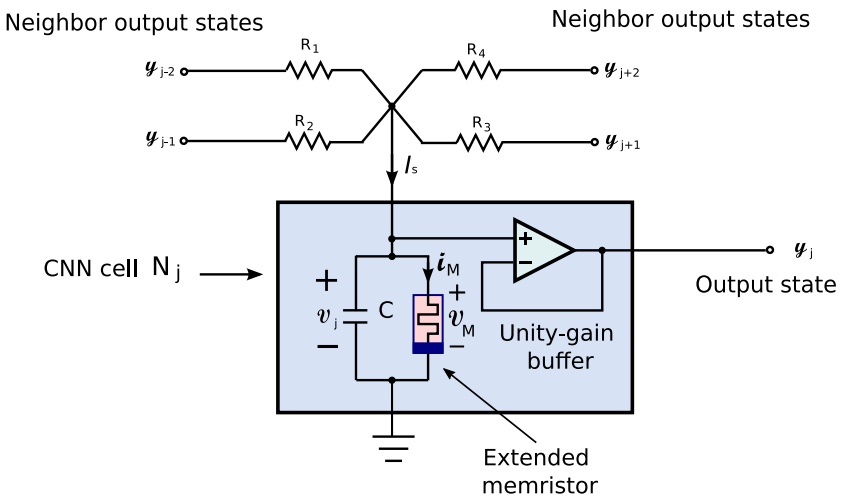

Figure 10: A memristor CNN cell model. The CNN cell N_j consists of three elements, that is, a capacitor C, a coupled extended memristor, and a unity-gain buffer, where $C = 1$ and $v_j = v_M = y_j$. The v-i characteristic of the coupled extended memristor is given by $i_M = -\left(\frac{a}{2\Delta x}\right)(y_{j+1} - y_{j-1})\, W(\varphi_j)\, v_M$, where φ_j is the flux of the coupled extended memristor and $W(\varphi_j)$ is a scalar function of φ $(= \int v_M(t)dt)$. Even though the extended memristor appears to be disconnected, its dynamics is coupled via the state variables y_{j+1} and y_{j-1}. Each CNN cell are connected to four neighbor cells using the four resistors $R_i (i = 1, 2, 3, 4)$. A unity gain buffer is an op-amp circuit which has a voltage gain of 1.

3.4.1 Computer simulations

Consider tthe Korteweg-de Vries (KdV) memristor CNN Diff. Eq. (92) with $N = 256$ (cells). Assume that the initial condition is given by the sine wave:

$$v_j^0 = \sin\left[2\pi\left(\frac{j}{N}\right)\right], \tag{94}$$

and the boundary condition is given by the periodic boundary condition:

$$\left.\begin{array}{rcl} v_0^n & = & v_N^n, \\ v_{-1}^n & = & v_{N-1}^n, \\ v_{N+1}^n & = & v_1^n, \\ v_{N+2}^n & = & v_2^n. \end{array}\right\} \tag{95}$$

We show our computer simulations in Fig. 11, where the parameters for Eq. (92) is given by

$$a = 0.2,\ b = 0.1,\ N = 256,\ \Delta t = 0.1,\ \Delta x = 0.4,\ n = 7000. \tag{96}$$

Observe that the initial sin wave evolves into a train of soliton waves. When a soliton interacts with another soliton, it emerges from the collision without a phase shift. Ultimately, the solution breaks down (that is, a floating point overflow occurs in our computer simulations). The three-dimensional plot of soliton waves looks like a *chicken cockscomb*.

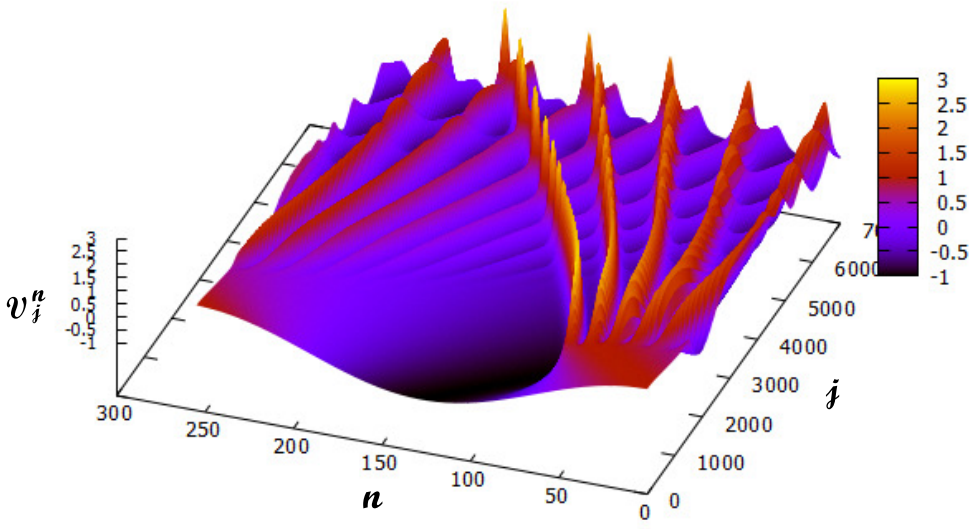

(a)

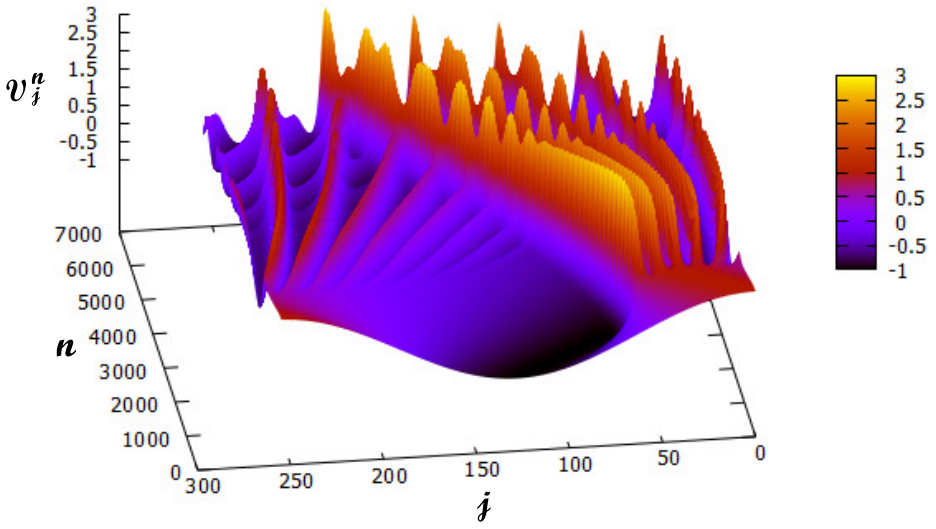

(b)

Figure 11: Three-dimensional plots of soliton waves in the Korteweg-de Vries (KdV) CNN Diff. Eq. (88). Two different plots of the soliton waves are shown. The initial condition is given by the sine wave and the boundary condition is given by the periodic boundary condition. The soliton waves of Fig. 11 (b) look like a *chicken cockscomb*.

Assume that the initial condition is given by the function of tangent hyperbolic:

$$v_j^0 = \frac{1 - \tanh\left(\dfrac{j-100)}{1.5}\right)}{2}; \tag{97}$$

and the boundary condition is given by the fixed boundary condition:

$$\left.\begin{array}{rcl} v_1^n & = & v_2^n = 1, \\ v_{N-1}^n & = & v_N^n = 0. \end{array}\right\} \tag{98}$$

We show our computer simulations in Fig. 12, where the parameters for Eq. (92) are given by

$$a = 0.5,\ b = 0.1,\ N = 256,\ \Delta t = 0.05,\ \Delta x = 0.3,\ 0 \le n \le 400. \tag{99}$$

Observe that the initial wave evolves into a train of soliton waves.

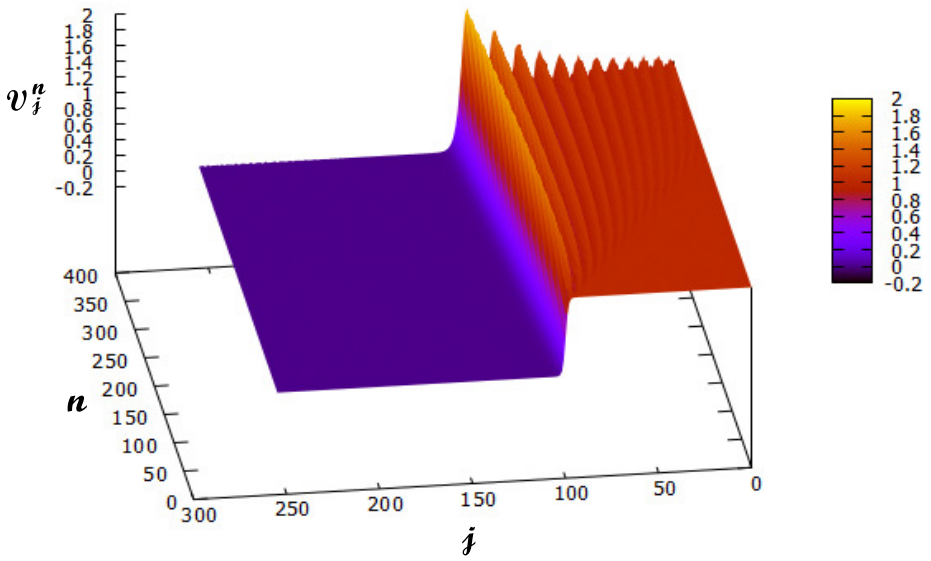

Figure 12: TThree-dimensional plots of soliton waves in the Korteweg-de Vries (KdV) CNN Diff. Eq. (88). The initial condition is given by the function of tangent hyperbolic and the boundary condition is given by the fixed boundary condition.

Consider next the Korteweg-de Vries (KdV) *memristor* CNN Diff. Eq. (92). Assume that the initial condition is given by

$$v_j^0 = \left|\cos\left[2\pi\left(\frac{j}{N}\right)\right]\right|, \tag{100}$$

and the boundary condition is given by the periodic boundary condition:

$$\left.\begin{array}{rcl} v_0^n & = & v_N^n, \\ v_{-1}^n & = & v_{N-1}^n, \\ v_{N+1}^n & = & v_1^n, \\ v_{N+2}^n & = & v_2^n. \end{array}\right\} \tag{101}$$

We show our computer simulations in Fig. 13, where the parameters for Eq. (92) are given by

$$a = 0.2,\ b = 0.1,\ N = 256,\ \Delta t = 0.05,\ \Delta x = 0.4,\ 0 \leq n \leq 40000. \tag{102}$$

and $W(\varphi_j)$ is given by

$$W(\varphi_j) = \left\{\begin{array}{ll} 1, & |\varphi| \leq 1, \\ 1.5, & \text{(otherwise)}, \end{array}\right. \tag{103}$$

where c and d are constants. Observe that the three-dimensional plot of the soliton waves exhibit more complicated (chaotic) behavior than that of the Korteweg-de Vries (KdV) CNN Diff. Eq. (88).

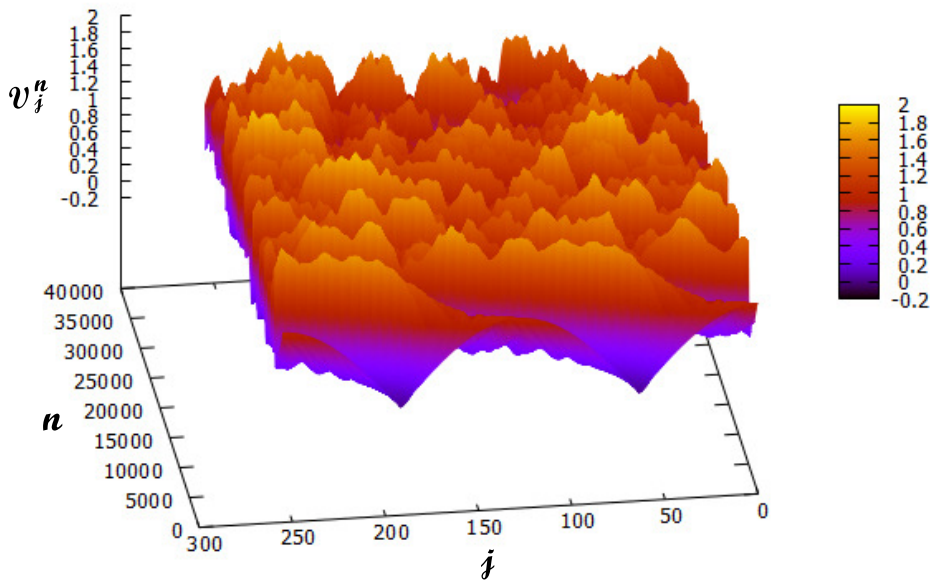

(a) three-dimensional plot

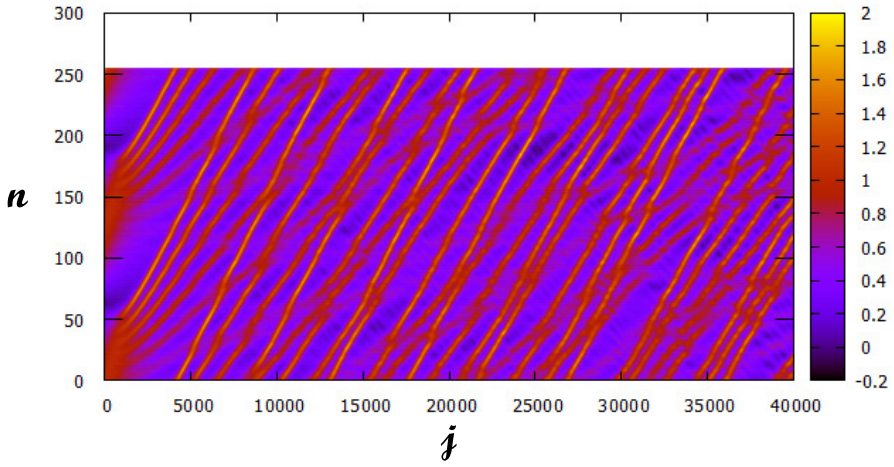

(b) two-dimensional plot

Figure 13: Two different views of the waves in the Korteweg-de Vries (KdV) memristor CNN Diff. Eq. (92). The initial condition is given by the cosine wave and the boundary condition is given by the periodic boundary condition. (a) Observe that the waves exhibit complicated (chaotic and distorted) behavior. (b) Observe that the wave interacts with another wave, and it emerges from the collision. In Fig. 13(b), the z-coordinate, that is, v_j^n is mapped onto a plane by projecting the three-dimensional plot along the z axis.

4 Sine-Gordon Equation

The sine-Gordon equation appears in a number of other physical applications, including the propagation of fluxons in Josephson junctions. The sine-Gordon equation is

$$\frac{\partial^2 u(x,t)}{\partial t^2} - \frac{\partial^2 u(x,t)}{\partial x^2} - \sin(u(x,t)) = 0, \tag{104}$$

where $u(x,t)$ is the amplitude of the wave at position x and time t, and a is the velocity of the wave.

4.1 Difference equation approximation

We approximate Eq. (104) by using the central difference scheme. Let us define u_j^n by

$$u_j^n \stackrel{\text{def}}{=} u(x_j, t_n), \tag{105}$$

where $x_j = x_0 + j\Delta x$ and $t_n = t_0 + n\Delta t$ (x_0, t_0, Δx, and Δt are some constants, and j and n are integers). Using the *second-order central difference* for the space and time derivatives, we obtain:

$$\begin{aligned} \left.\frac{\partial^2 u(x,t)}{\partial x^2}\right|_{t=t_n,\, x=x_j} &\approx \frac{u_{j+1}^n - 2u_j^n + u_{j-1}^n}{(\Delta x)^2}, \\ \left.\frac{\partial^2 u(x,t)}{\partial t^2}\right|_{t=t_n,\, x=x_j} &\approx \frac{u_j^{n+1} - 2u_j^n + u_j^{n-1}}{(\Delta t)^2}, \end{aligned} \tag{106}$$

where $|\Delta x|$ and $|\Delta t|$ are sufficiently small. Substituting Eq. (106) into Eq. (104), we obtain

$$\frac{u_{j+1}^n - 2u_j^n + u_{j-1}^n}{(\Delta t)^2} - \frac{u_{j+1}^n - 2u_j^n + u_{j-1}^n}{(\Delta x)^2} - \sin(u_j^n) = 0. \tag{107}$$

It can be recast into the form

$$u_{j+1}^n = 2u_j^n - u_{j-1}^n + \frac{(\Delta t)^2}{(\Delta x)^2}(u_{j+1}^n - 2u_j^n + u_{j-1}^n) + (\Delta t)^2 \sin(u_j^n). \tag{108}$$

4.2 Boundary condition setting

Consider the difference equation (108) with N cells. The boundary conditions in Sec. 2.1.2 are described as follow:

- Dirichlet (fixed) boundary condition:

$$\left.\begin{aligned} u_1^n &= f(x_1), \\ u_N^n &= f(x_N). \end{aligned}\right\} \tag{109}$$

- Periodic boundary condition:

$$\left.\begin{aligned} u_0^n &= u_N^n \\ u_{N+1}^n &= u_1^n \end{aligned}\right\} \tag{110}$$

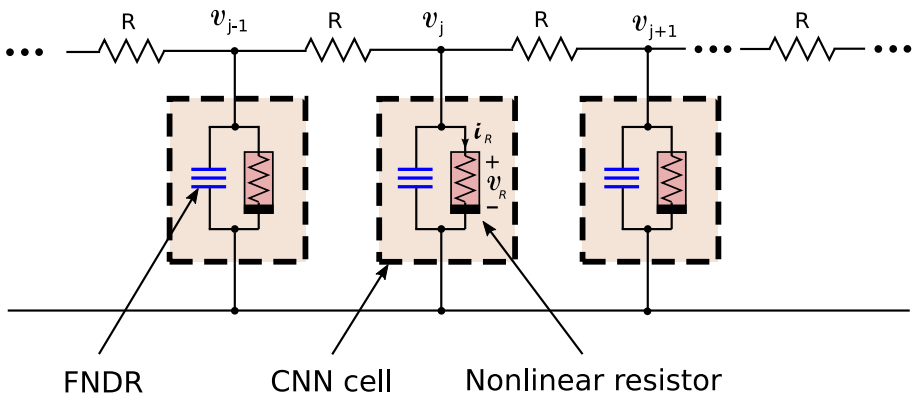

Figure 14: A CNN realization of Eq. (108) with linear resistor coupling between cells. The CNN cell consists of a FNDR and a nonlinear resistor described by $i_R = \sin(v_R)$.

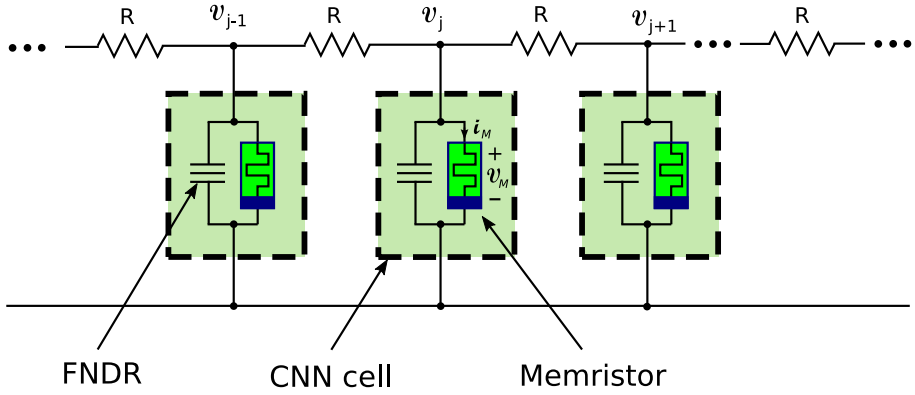

Figure 15: A CNN realization of Eq. (108) with linear resistor coupling between cells. The CNN cell consists of a FNDR described by $q = G(d^2\varphi/dt^2)$ and a memristor described by a constitutive relation between the charge q and the flux φ, that is, $q = \sin(\varphi)$. Differentiate both sides of $q = \sin(\varphi)$ with respect to t, we can obtain the relation between the terminal voltage v_M and terminal current i_M, that is, $i_M = \cos(\varphi)v_M$ ($i_M = \frac{dq}{dt}$, $v_M = \frac{d\varphi}{dt}$).

4.2.1 CNN circuit realization and difference equation approximation

We show the circuit realization of Eq. (108). Consider the resistor-coupled CNN shown in Fig. 14.[5] The dynamics of this circuit is given by

$$\frac{d^2v_j(t)}{dt^2} = \frac{1}{R}\left(v_{j+1}(t) - 2v_j(t) + v_{j-1}(t)\right) + \sin(v_j(t)). \tag{111}$$

If we replace the voltage $v_j(t)$ in Eq. (111) with the flux $\varphi_j(t)$, we obtain

$$\frac{d^2\varphi_j(t)}{dt^2} = \frac{1}{R}\left(\varphi_{j+1}(t) - 2\varphi_j(t) + \varphi_{j-1}(t)\right) + \sin(\varphi_j(t)). \tag{112}$$

Equation (112) can be realized by the memristor circuit in Fig. 15.

[5]The FNDR is defined by $i = G(d^2v/dt^2)$ in Sec. 2.1. However, in Fig. 14, the FNDR is described by $q = G(d^2\varphi/dt^2)$. Differentiating this equation with respect to t, we obtain $i = G(d^2v/dt^2)$, where $i = dq/dt$ and $v = d\varphi/dt$. Thus, these two equations are identical.

Consider Eq. (111). Let $v_j^n = v_j(t_n)$, where $t_n = t_0 + n\Delta t$. Using the second-order central difference for the time derivative:

$$\left.\frac{d^2 v_j(t)}{dt^2}\right|_{t=t_n} \approx \frac{v_j^{n+1} - 2v_j^n + v_j^{n-1}}{(\Delta t)^2}, \tag{113}$$

we obtain the following difference equation from Eq. (111):

$$\frac{v_j^{n+1} - 2v_j^n + v_j^{n-1}}{(\Delta t)^2} = \frac{1}{R}\left(v_{j+1}^n - 2v_j^n + v_{j-1}^n\right) + \sin(v_j^n). \tag{114}$$

where Δt is sufficiently small. It can be recast into the form

$$v_{j+1}^n = 2v_j^n - u_{j-1}^n + \frac{(\Delta t)^2}{(\Delta x)^2}(v_{j+1}^n - 2v_j^n + v_{j-1}^n) + (\Delta t)^2 \sin(v_j^n), \tag{115}$$

where we set $R = (\Delta x)^2$. Thus, Eq. (115) is equivalent to Eq. (108), that is, they have the same solution. We call Eq. (115) as the Sine-GordonCNN Diff. Eq.

Similarly, from Eq. (112), we obtain

$$\varphi_{j+1}^n = 2\varphi_j^n - \varphi_{j-1}^n + \frac{(\Delta t)^2}{(\Delta x)^2}(\varphi_{j+1}^n - 2\varphi_j^n + \varphi_{j-1}^n) + (\Delta t)^2 \sin(\varphi_j^n), \tag{116}$$

where $\frac{d\varphi_j^n}{dt} = v_j^n$. It goes without saying that Eq. (116) is to equivalent to Eqs. (108) and (115), that is, they have the same solution. We call Eq. (116) as the sine-Gordon memristor CNN Diff. Eq.

4.2.2 Computer simulations

Consider the sine-Gordon memristor CNN Diff. Eq. (116) with $N = 200$ (cells). Assume that the initial condition is given by the pulse with the height of 30:

$$\varphi_j^0 = \begin{cases} 30 & (50 \le j \le 70), \\ 0 & (\text{otherwise}), \end{cases} \tag{117}$$

and the boundary condition is given by the Dirichlet (fixed) boundary condition:

$$\left.\begin{array}{rcl} \varphi_1^n & = & 0, \\ \varphi_N^n & = & 0, \end{array}\right\} \tag{118}$$

where $j = 1, 2, \cdots, 200$. We show our computer simulations in Fig. 16, where the parameters for Eq. (116) are given by

$$N = 200,\ \Delta t = 0.1,\ \Delta x = 0.1,\ 0 \le n \le 398. \tag{119}$$

From our computer simulations, we observed the following behavior:

- The three dimensional plot of the solutions is little *distorted*, compared with that of the second-order linear wave CNN Diff. Eq. (27) (see Fig 2 (b)).
- The solitary wave moves at *constant speed*. Furthermore, the wave with a negative amplitude (blue) interacts with another wave ($n \approx 199$), and it emerges from the collision.
- The solution returns the state which is roughly similar to the initial pulse ($n = 398$), that is, the *recurrence of the initial state* is observed.

Let us next replace the sine function $\sin(\varphi_j^n)$ in Eq. (116) with the simple *signum* function, which is defined by

$$\mathrm{sgn}(\varphi_j^n) = \begin{cases} -1 & \text{if} \quad \varphi_j^n < 0, \\ 0 & \text{if} \quad \varphi_j^n = 0, \\ 1 & \text{if} \quad \varphi_j^n > 0. \end{cases} \tag{120}$$

The initial condition is given by Eq. (117) and the boundary condition is given by Eq. (118). Then we obtain the results in Fig. 17. Observe that the three dimensional plot of the solution is much more distorted in the neighborhood of $n = 398$. Thus, we conclude that the nonlinear term $\sin(\varphi_j^n)$ or the piecewise linear term $\mathrm{sgn}(\varphi_j^n)$ causes the distortion in the wave.

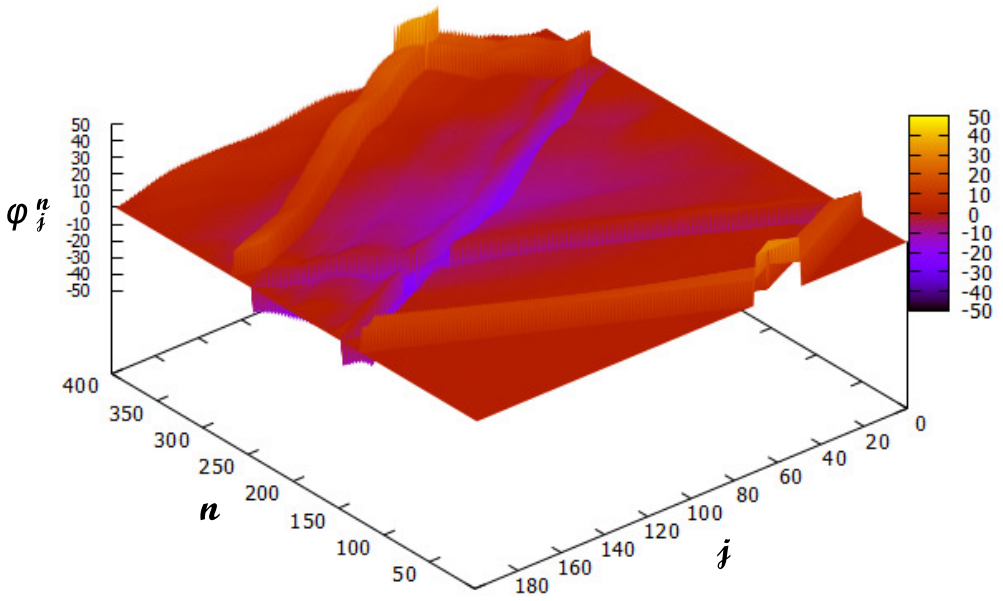

(a) three-dimensional plot

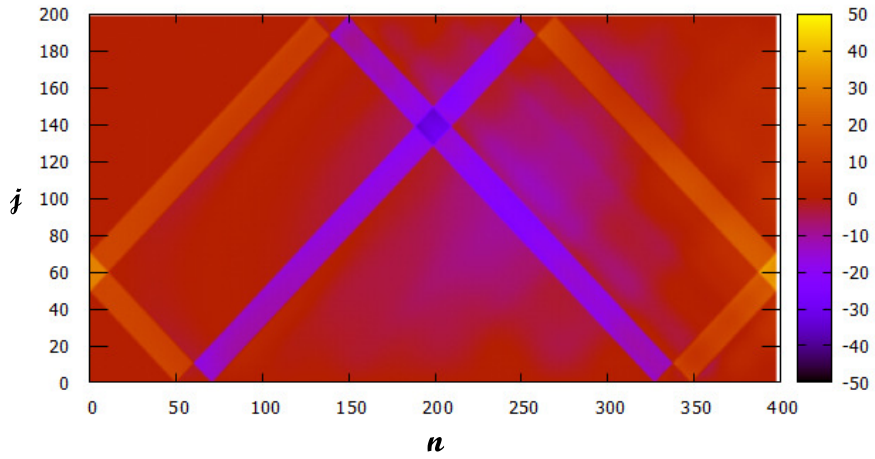

(b) two-dimensional plot

Figure 16: Two different views of the waves in the sine-Gordon memristor CNN Diff. Eq. (116). The initial condition is given by the pulse with the height of 30 and the boundary condition is given by the Dirichlet (fixed) boundary condition. (a) Observe that the three dimensional plot of the solution is little distorted, compared with that of Fig. 2 (b). Note that the solution returns the state which is roughly similar to the initial pulse ($n = 398$). (b) Observe that the wave moves at constant speed. Furthermore, the wave with a negative amplitude (blue) interacts with another wave ($n \approx 199$), and it emerges from the collision. In this figure, the z-coordinate, that is, φ_j^n is mapped onto a plane by projecting the three-dimensional plot along the z axis.

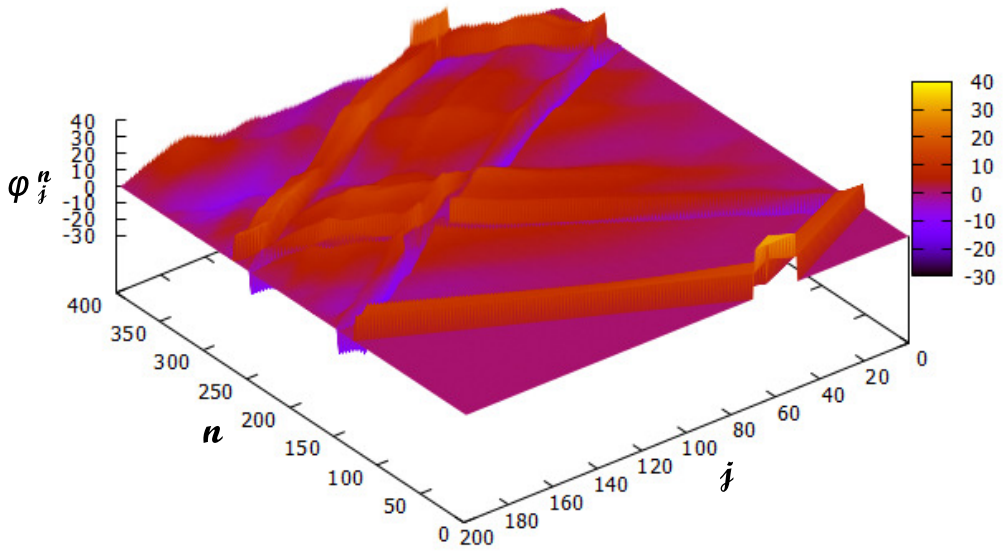

(a) three-dimensional plot

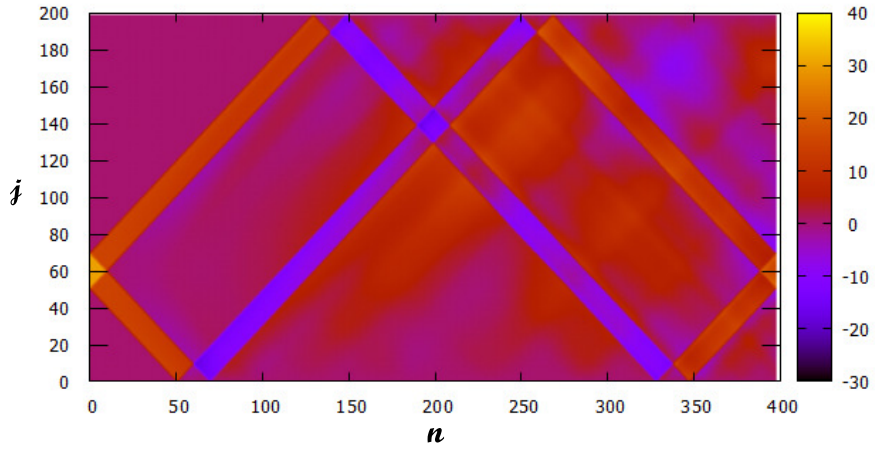

(b) two-dimensional plot

Figure 17: Two different views of the waves in the sine-Gordon memristor CNN Diff. Eq. (116), in which the sine function is replaced by the *signum* function. The initial condition is given by the pulse with the height of 30 and the boundary condition is given by the Dirichlet (fixed) boundary condition. (a) Observe that the three dimensional plot of the solution is much more distorted, compared with that of Fig. 2 (b). (b) Observe that the wave movies at constant speed. Furthermore, the wave with a negative amplitude (blue) interacts with another wave ($n \approx 199$), and it emerges from the collision. In this figure, the z-coordinate, that is, φ_j^n is mapped onto a plane by projecting the three-dimensional plot along the z axis.

5 Toda Lattice Equation

The Toda lattice is a simple model for a one-dimensional crystal in solid state physics. The Hamiltonian of such a system is given by [7, 8]

$$\mathcal{H} = \sum_j \frac{1}{2} {p_j}^2 + \sum_j e^{-(\,q_{j+1}-q_j\,)} \tag{121}$$

where q_j is the displacement of the j-th particle from its equilibrium position, and p_j is its momentum (mass $m = 1$). Then, the Hamilton's Equations are given by

$$\left.\begin{array}{rcl} \dfrac{dq_j}{dt} &=& p_j, \\ \dfrac{dp_j}{dt} &=& e^{-(\,q_j-q_{j-1}\,)} - e^{-(\,q_{j+1}-q_j\,)}, \end{array}\right\} \tag{122}$$

where $j = 1,\ 2, \cdots,\ N$ and we consider the case of a periodic lattice of the length N: $q_j = q_{j+N}$.

Define new variables

$$\left.\begin{array}{rcl} a_j &=& \dfrac{1}{2} e^{-(\,q_{j+1}-q_j\,)/2}, \\ b_j &=& \dfrac{1}{2} p_j, \end{array}\right\} \tag{123}$$

where $j = 1,\ 2, \cdots,\ N$. Then Eq.(122) can be recast into the form [8, 9]

$$\left.\begin{array}{rcl} \dfrac{da_j(t)}{dt} &=& (b_j(t) - b_{j+1}(t))a_j(t), \\ \dfrac{db_j(t)}{dt} &=& 2\,(a_{j-1}(t)^2 - a_j(t)^2), \end{array}\right\} \tag{124}$$

where $j = 1,\ 2, \cdots,\ N$. In the case of a periodic lattice of the length N, $a_j = a_{j+N}$, $b_j = b_{j+N}$.

5.1 Difference equation approximation

We approximate Eq. (124) by using the central difference scheme. Let us define a_j^n and b_j^n by

$$\left.\begin{array}{l} a_j^n \stackrel{\text{def}}{=} a_j(t_n), \\ b_j^n \stackrel{\text{def}}{=} b_j(t_n). \end{array}\right\} \tag{125}$$

where $t_n = t_0 + n\Delta t$ (t_0 and Δt are some constants). Using the *second-order central difference* for the space and time derivatives, we obtain

$$\left.\begin{array}{rcccl} \left.\dfrac{da_j(t)}{dt}\right|_{t=t_n} &\approx& \dfrac{a_j(t_{n+2}) - a_j(t_n)}{2\Delta t} &=& \dfrac{a_j^{n+2} - a_j^n}{2\Delta t}, \\ \left.\dfrac{db_j(t)}{dt}\right|_{t=t_n} &\approx& \dfrac{b_j(t_{n+2}) - b_j(t_{n+2})}{2\Delta t} &=& \dfrac{b_j^{n+2} - b_j^n}{2\Delta t}, \end{array}\right\} \tag{126}$$

where Δt is sufficiently small. Then, we can approximate Eq. (124) by the following difference equation:

$$\left.\begin{array}{rcl} \dfrac{a_j^{n+2} - a_j^n}{2\Delta t} &=& \Big(b_j^n - b_{j+1}^n\Big)a_j^n, \\ \dfrac{b_j^{n+2} - b_j^n}{2\Delta t} &=& 2\,\Big((a_{j-1}^n)^2 - (a_j^n)^2\Big), \end{array}\right\} \tag{127}$$

It can be recast into the form

$$\left.\begin{aligned} a_j^{n+2} &= a_j^n + 2\Delta t \left(b_j^n - b_{j+1}^n\right) a_j^n, \\ b_j^{n+2} &= b_j^n + 2\Delta t \left((a_{j-1}^n)^2 - (a_j^n)^2\right). \end{aligned}\right\} \tag{128}$$

We call Eq. (128) as the Toda lattice Diff. Eq.

5.2 Boundary condition setting

Consider the Toda lattice Diff. Eq. (128) with N cells. The boundary conditions in Sec. 2.1.2 are described as follow:

- Dirichlet (fixed) boundary condition:

$$\left.\begin{aligned} a_1^n &= a_2^n &&= f(x_1), \\ a_{N-1}^n &= a_N^n &&= f(x_N), \\ b_1^n &= b_2^n &&= g(x_1), \\ b_{N-1}^n &= b_N^n &&= g(x_N), \end{aligned}\right\} \tag{129}$$

- Periodic boundary condition:

$$\left.\begin{aligned} a_0^n &= a_N^n, \\ a_{-1}^n &= a_{N-1}^n, \\ b_0^n &= b_N^n. \end{aligned}\right\} \tag{130}$$

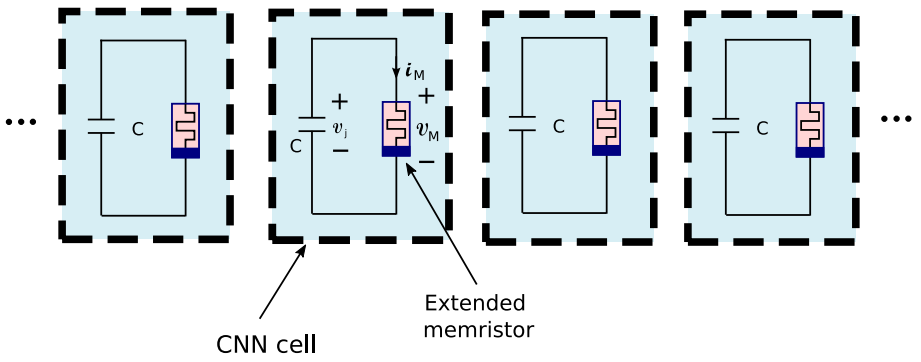

Figure 18: A CNN realization of Eq. (128). The CNN cell consists of a capacitor and a coupled extended memristor. The v-i characteristic of the coupled extended memristor is given by $i_M = (x_j - x_{j+1})v_M$, $\frac{dx_j}{dt} = 2({v_{j-1}}^2 - {v_j}^2)$, where $v_M = v_j$ and $C = 1$. Even though the extended memristor appear to be disconnected, their dynamics are coupled wit the state variables.

5.3 CNN circuit realization and difference equation approximation

We show the circuit realization of Eq. (128). Consider the circuit shown in Fig. 18. The dynamics of this circuit is given by

$$\begin{aligned} \frac{dv_j}{dt} &= (x_j - x_{j+1})v_j, \\ \frac{dx_j}{dt} &= 2({v_{j-1}}^2 - {v_j}^2), \end{aligned} \tag{131}$$

where the coupled extended memristor is defined by

$$\begin{aligned} i_M &= (x_j - x_{j+1})v_M, \\ \frac{dx_j}{dt} &= 2({v_{j-1}}^2 - {v_j}^2), \end{aligned} \tag{132}$$

where $C = 1$ and $v_M = v_j$.

Let $v_j(t_n) = v_j^n$, where $t_n = t_0 + n\Delta t$. Using the *second-order central difference* for the time derivative, we obtain

$$\left.\begin{aligned} \left.\frac{dv_j(t)}{dt}\right|_{t=t_n} &\approx \frac{v_j(t_{n+2}) - v_j(t_n)}{2\Delta t} = \frac{v_j^{n+2} - v_j^n}{2\Delta t}, \\ \left.\frac{dx_j(t)}{dt}\right|_{t=t_n} &\approx \frac{x_j(t_{n+2}) - x_j(t_{n+2})}{2\Delta t} = \frac{x_j^{n+2} - x_j^n}{2\Delta t}, \end{aligned}\right\} \tag{133}$$

where Δt is sufficiently small. Then, we can approximate Eq. (131) by the following difference equation:

$$\left.\begin{aligned} \frac{v_j^{n+2} - v_j^n}{2\Delta t} &= \left(x_j^n - x_{j+1}^n\right)v_j^n, \\ \frac{x_j^{n+2} - x_j^n}{2\Delta t} &= 2\left((v_{j-1}^n)^2 - (v_j^n)^2\right). \end{aligned}\right\} \tag{134}$$

It can be recast into the form

$$\left.\begin{aligned} v_j^{n+2} &= v_j^n + 2\Delta t\left(x_j^n - x_{j+1}^n\right)v_j^n, \\ x_j^{n+2} &= x_j^n + 4\Delta t\left((v_{j-1}^n)^2 - (v_j^n)^2\right). \end{aligned}\right\} \tag{135}$$

Thus, Eq. (135) is equivalent to Eq. (128), that is, they have the same solution. We call Eq. (135) as the Toda lattice memristor CNN Diff. Eq.

5.3.1 Computer simulations

Assume that the initial condition is given by the sine wave:

$$\left.\begin{aligned} v_j^0 &= 0.01\left(1.5 - \sin\left[2\pi\left(\frac{j-1}{N}\right)\right]\right), \\ x_j^0 &= 0.02\, v_j^0. \end{aligned}\right\} \tag{136}$$

Furthermore, in order to calculate v_j^n and x_j^n for $n = 2, 3, \cdots$ from Eq. (135), we need to know v_j^1 and x_j^1. Using the *forward (two-point) difference*, we obtain

$$\left.\begin{aligned} \left.\frac{dv_j}{dt}\right|_{t=t_0} &\approx \frac{v_j(t_1) - v_j(t_0)}{\Delta t} = \frac{v_j^1 - v_j^0}{\Delta t}, \\ \left.\frac{dx_j}{dt}\right|_{t=t_0} &\approx \frac{x_j(t_1) - x_j(t_0)}{\Delta t} = \frac{x_j^1 - x_j^0}{\Delta t}. \end{aligned}\right\} \tag{137}$$

where $\Delta t = t_1 - t_0$ is sufficiently small. Then, we can approximate Eq. (131) by

$$\left.\begin{array}{rcl} \dfrac{v_j^1 - v_j^0}{\Delta t} & = & \Big(x_j^0 - x_{j+1}^0\Big) v_j^0, \\ \dfrac{x_j^1 - x_j^0}{\Delta t} & = & 2\Big((v_{j-1}^0)^2 - (v_j^0)^2\Big). \end{array}\right\} \tag{138}$$

It can be recast into the form:

$$\left.\begin{array}{rcl} v_j^1 & = & v_j^0 + \Delta t \Big(x_j^0 - x_{j+1}^0\Big) v_j^0, \\ x_j^1 & = & x_j^n + 2\Delta t \Big((v_{j-1}^0)^2 - (v_j^0)^2\Big), \end{array}\right\} \tag{139}$$

Thus, we can obtain v_j^1 and x_j^1 using the initial conditions x_j^0, x_{j+1}^0, v_j^0, and v_{j-1}^0. Assume next that the boundary condition is given by the periodic boundary condition:

$$\left.\begin{array}{rcl} v_0^n & = & v_N^n, \\ v_{-1}^n & = & v_{N-1}^n, \\ x_0^n & = & x_N^n. \end{array}\right\} \tag{140}$$

We show our computer simulations in Fig. 19, where $\Delta t = 0.1$ and $N = 256$. Observe that the Toda lattice memristor CNN Diff. Eq. (135) exhibits the following soliton-like behavior:

- The shape of the initial curve is distorted continuously with increasing time.
- The wave moves to the boundary, and reflects back. Then, the wave gets progressively steeper.
- *A train of solitary waves* are generated from the steepest part of the distorted wave. They move to the boundary, and reflect back.
- A train of reflected solitary waves with negative (res. positive) amplitude interact with a train of solitary waves with a positive (res. negative) amplitude, and they emerge from the collisions.
- After a certain period of time, the solution breaks down (a floating point overflow occurs in our computer simulations).

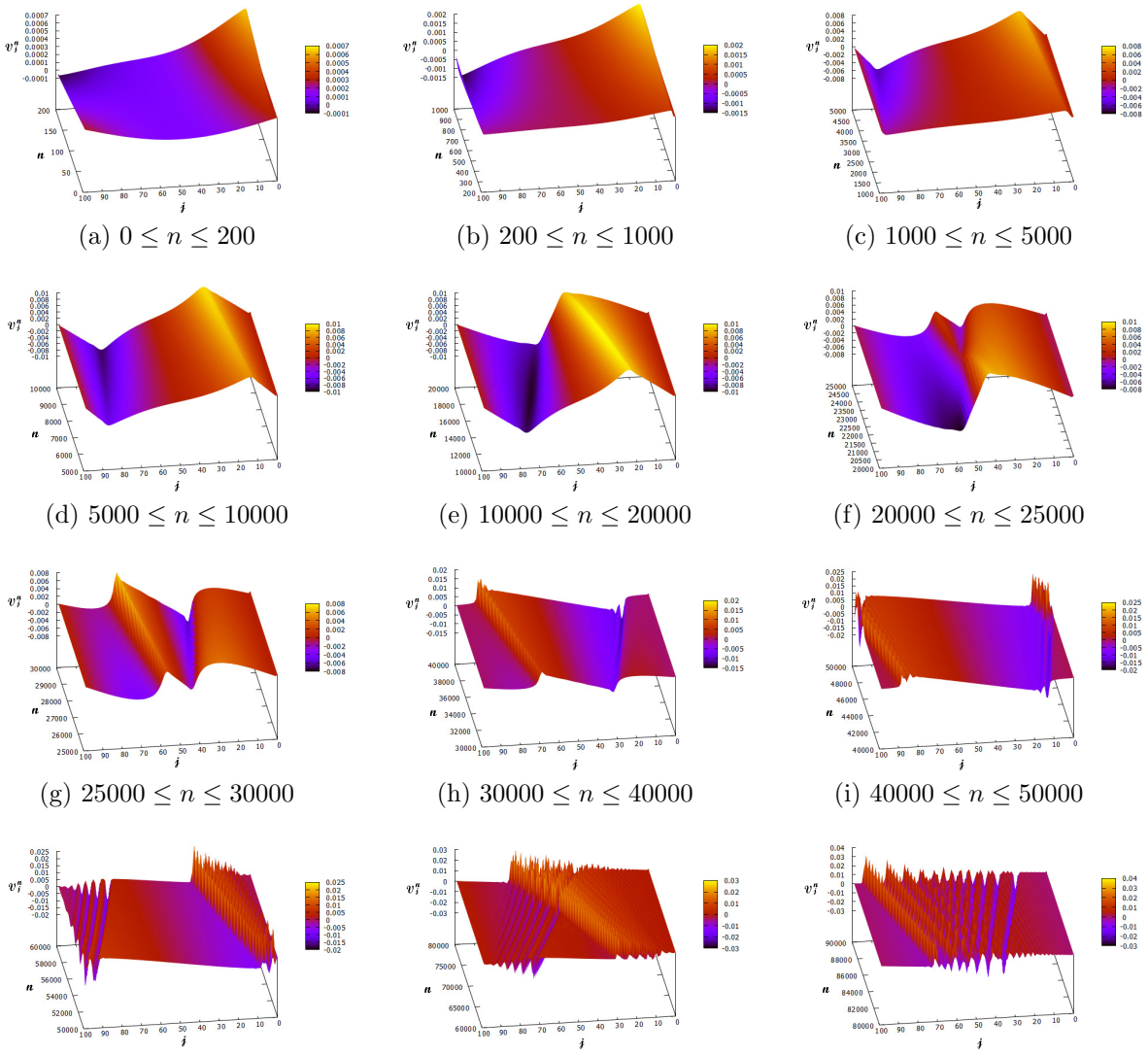

(a) $0 \leq n \leq 200$ (b) $200 \leq n \leq 1000$ (c) $1000 \leq n \leq 5000$

(d) $5000 \leq n \leq 10000$ (e) $10000 \leq n \leq 20000$ (f) $20000 \leq n \leq 25000$

(g) $25000 \leq n \leq 30000$ (h) $30000 \leq n \leq 40000$ (i) $40000 \leq n \leq 50000$

(j) $50000 \leq n \leq 60000$ (k) $60000 \leq n \leq 80000$ (l) $80000 \leq n \leq 90000$

Figure 19: Three-dimensional plots of soliton waves in the Toda lattice memristor CNN Diff. Eq. (135). The initial condition is given by the sine wave and the boundary condition is given by the periodic boundary condition. (a)-(g) The shape of the initial curve is distorted continuously with increasing time. (h)-(j) A train of solitary waves are generated from the steepest part of the distorted wave. (k)-(l) A train of solitary waves with *negative* (res. positive) amplitude interact with a train of solitary waves with a *positive* (res. negative) amplitude, and they emerge from the collisions.

6 Conclusion

We have studied the solitary waves in the CNN difference equations. A remarkable point is that the second-order linear wave CNN difference equation can exhibit the basic properties of solitons. We have also shown that the solitons in the memristor CNN difference equations exhibit more complicated behavior. In this paper, we used the central difference scheme for solving the differential equations. If we use other difference schemes, we may observe more interesting behavior. Furthermore, we used the synchronous parallel model to obtain the solutions of the CNN difference equations. If we use the sequential model, then we may obtain similar but little different results.

References

[1] Zabusky, N.J. and Porter, M.A.(2010) Soliton, Scholarpedia, 5(8):2068.

[2] Chua L.O., Hasler M., Moschytz G.S., and Neirynsk J. (1995) Autonomous Cellular Neural Networks: A Unified Paradigm for Pattern Formation and Active Wave Propagation, *IEEE Trans. CAS-I*, **42**(10), 559-577.

[3] Itoh, M.(2019) Nonlinear Waves in Two-Dimensional Autonomous Cellular Neural Networks Coupled by Memristors, viXra:1912.0197 [Category: Mathematical Physics].

[4] Itoh, M.(2020) Complex Nonlinear Waves in Autonomous CNNs Having Two Layers of Memristor Couplings, viXra:2004.0241 [Category: Mathematical Physics].

[5] Itoh, M.(2019b) Memristor Circuit Equations with Periodic Forcing, viXra:1902.0345 [Category: Mathematical Physics].

[6] Korteweg, D.J. and de Vries, F.(1895) On the Change of Form of Long Waves Advancing in a Rectangular Canal, and on a New Type of Long Stationary Waves, Philos. Mag. **39**, 422-443.

[7] Toda, M. (1986) *Non-linear wave and soliton* (in Japanese) (Nihon-hyouron-sha, Tokyo).

[8] Toda, M. (1989) *Theory of Nonlinear Lattices (2nd ed.)* (Springer, Berlin).

[9] Teschl, G. (2001) Almost everything you always wanted to know about the Toda equation. Jahresber. Deutsch. Math.-Verein. **103**(4), 149-162.